

9-1996

The Peculiar Motions of Early-Type Galaxies in Two Distant Regions. I. Cluster and Galaxy Selection

Gary Wegner
Dartmouth College

Matthew Colless
Australian National University

Glenn Baggley
University of Durham

Roger L. Davies
University of Durham

Follow this and additional works at: <https://digitalcommons.dartmouth.edu/facoa>



Part of the [External Galaxies Commons](#)

Recommended Citation

Wegner, Gary; Colless, Matthew; Baggley, Glenn; and Davies, Roger L., "The Peculiar Motions of Early-Type Galaxies in Two Distant Regions. I. Cluster and Galaxy Selection" (1996). *Open Dartmouth: Faculty Open Access Articles*. 2309.
<https://digitalcommons.dartmouth.edu/facoa/2309>

This Article is brought to you for free and open access by Dartmouth Digital Commons. It has been accepted for inclusion in Open Dartmouth: Faculty Open Access Articles by an authorized administrator of Dartmouth Digital Commons. For more information, please contact dartmouthdigitalcommons@groups.dartmouth.edu.

THE PECULIAR MOTIONS OF EARLY-TYPE GALAXIES IN TWO DISTANT REGIONS. I. CLUSTER AND GALAXY SELECTION

GARY WEGNER

Department of Physics and Astronomy, 6127 Wilder Laboratory, Dartmouth College, Hanover, NH 03755-3528

MATTHEW COLLESS

Mount Stromlo and Siding Spring Observatories, Australian National University, Weston Creek, ACT 2611, Australia

GLENN BAGGLEY AND ROGER L. DAVIES

Department of Physics, University of Durham, South Road, Durham DH1 3LE, England

EDMUND BERTSCHINGER

Department of Physics, MIT 6-207, Massachusetts Institute of Technology, Cambridge, MA 02139

DAVID BURSTEIN

Department of Physics and Astronomy, Box 871054, Arizona State University, Tempe, AZ 85287-1504

ROBERT K. MCMAHAN, JR.¹

Department of Physics and Astronomy, University of North Carolina, CB 3255 Phillips Hall, Chapel Hill, NC 27599-3255

AND

R. P. SAGLIA

Universitäts-Sternwarte München, Scheinerstraße 1, D-81679 München, Germany

Received 1995 September 18; accepted 1996 February 29

ABSTRACT

The EFAR project is a study of 736 candidate elliptical galaxies in 84 clusters lying in two regions, toward Hercules–Corona Borealis and Perseus–Pisces–Cetus, at distances $cz \approx 6000$ – $15,000 \text{ km s}^{-1}$. In this paper (the first of a series), we present an introduction to the EFAR project and describe in detail the selection of the clusters and galaxies in our sample. Fundamental data for the galaxies and clusters are given, including accurate new positions for each galaxy and redshifts for each cluster. The galaxy selection functions are determined by using diameters measured from Schmidt sky survey images for 2185 galaxies in the cluster fields. Future papers in this series will present the spectroscopic and photometric observations of this sample, investigate the properties of the fundamental plane for elliptical galaxies, and determine the large-scale peculiar velocity fields in these two regions of the universe.

Subject headings: galaxies: clusters: general — galaxies: distances and redshifts — galaxies: elliptical and lenticular, cD — surveys

1. INTRODUCTION

This paper is the first in a series reporting the results of the EFAR project, studying the properties and peculiar motions of elliptical galaxies and clusters in two volumes of the universe at distances between 6000 and $15,000 \text{ km s}^{-1}$. The aims of this extensive observational program are (1) to study the intrinsic properties of elliptical galaxies in clusters by compiling a large and homogeneous sample with high-quality photometric and spectroscopic data, (2) to test possible systematic errors, such as environmental dependence, in existing elliptical galaxy distance estimators, (3) to seek improved distance estimators based on a more comprehensive understanding of the properties of elliptical galaxies and how these are affected by the cluster environment, and (4) to determine the peculiar velocity field in regions that are dynamically independent of the mass concentrations within 6000 km s^{-1} in order to test whether the large-amplitude coherent flows seen locally are typical of bulk motions in the universe.

The EFAR project was conceived in 1986 as a natural progression from the work of the Seven Samurai (“7S”; Dressler et al. 1987a; Lynden-Bell et al. 1988), who studied the peculiar velocity field traced by elliptical galaxies closer than 6000 km s^{-1} . The major finding of that work was that

the local region of the universe was dominated by large-scale, large-amplitude coherent motions. This result has been substantially confirmed both by further analysis (Faber & Burstein 1988; Bertschinger et al. 1990) and by subsequent observational studies, most of which employed the independent Tully–Fisher distance estimator for spiral galaxies (Aaronson et al. 1986, 1989; Han & Mould 1990; Willick 1990, 1991; Mathewson, Ford, & Buchhorn 1992; Mould et al. 1993; Courteau et al. 1993; Mathewson & Ford 1994). Although something is known about the peculiar velocity field within 6000 km s^{-1} , the nature of the mass concentrations that cause the flow remains controversial (see reviews by Bertschinger 1990; Burstein 1990; Dekel 1994; Strauss & Willick 1995), and relatively little is known about galaxy motions far away.

Initial comparisons of the velocity field with predictions of cosmological models (Vittorio, Juszkiewicz, & Davis 1986; Bertschinger & Juszkiewicz 1988) suggested that the observed motions were difficult to reconcile with the favored biased cold dark matter (CDM) models that they considered. The immediate question raised was whether the local volume was indeed typical of other regions of the universe (implying that the standard cosmological models were incorrect) or whether the local motions were merely an unusual statistical fluctuation in the universal velocity field. More recent analyses (Kaiser 1988, 1991; Feldman & Watkins 1994; Seljak & Bertschinger 1994; Dekel et al.

¹ Postal address: McMahan Research Laboratories, P.O. Box 14026, 79 Alexander Drive, Research Triangle, NC 27709.

1996) suggest that the local motions are consistent with the COBE-normalized standard CDM model. Nonetheless, whether or not the local motions are typical of the universe at large remains an important question. In order to answer this, we are measuring the peculiar motions in similarly large regions at sufficient distances to be dynamically independent of the local volume studied by 7S and most other workers.

During the period it has taken to complete the EFAR observing program, however, a wider variety of questions has arisen. Chief among these has been a more searching inquiry as to the reliability of the D_n - σ distance indicator developed by 7S (Dressler et al. 1987b; Lynden-Bell et al. 1988) and the physical origin of the fundamental plane (FP) of elliptical galaxies (Djorgovski & Davis 1987; Bender, Burstein, & Faber 1992; Saglia, Bender, & Dressler 1993a; Jørgensen, Franx, & Kjørgaard 1993; Pahre, Djorgovski, & de Carvalho 1995), of which it is simply a convenient projection. Various authors have suggested that there may be variations in the FP that correlate with galaxy environment, either directly, through mechanisms such as tidal stripping (Silk 1989), or indirectly, via different stellar populations (Gregg 1992, 1995). Such effects could lead to significant systematic errors in any distance estimators based on the FP relations. Some claims have been made for the detection of such variations (de Carvalho & Djorgovski 1992; Guzman & Lucey 1993). Other studies, however, find little variation of the FP with environment (Lynden-Bell et al. 1988; Burstein, Faber, & Dressler 1990; Lucey et al. 1991), and comparisons of FP and D_n - σ distance estimates with those derived from relatively independent and perhaps more accurate estimators, such as the Tully-Fisher and surface brightness fluctuation methods, show good agreement (Jacoby et al. 1992).

These concerns, and the focus they bring on the formation and evolution of the elliptical galaxy population, have become as important a motivation for this work as the original goal of measuring the peculiar velocity field at large distances. The EFAR project's goal of measuring the peculiar motions of *distant* elliptical galaxies from a *large* and *homogeneous* sample provides a test of the FP distance estimators that is both *severe* (since systematic errors in peculiar velocities are amplified at large distances) and *fair* (given the difficulties of comparing the FP for differently selected samples observed in different studies). It is worth noting that the 7S data set is still the largest in the literature for elliptical galaxies, though it was obtained a decade ago and is based on photoelectric aperture photometry and IDS spectroscopy. The EFAR sample is comparable in size to that of 7S and is based largely on CCD imaging and spectroscopy, which confer a number of advantages in the attempt to reduce observational errors.

Even if *systematic* errors prove negligible, the relatively large ($\sim 20\%$) *random* errors in the D_n - σ and Tully-Fisher distance estimators limit exploration of the velocity field beyond $\sim 6000 \text{ km s}^{-1}$ (the "local" region). The only studies that have attempted to measure the velocity field as far out as $15,000 \text{ km s}^{-1}$ are those of Lauer & Postman (1994), using brightest cluster galaxies as distance estimators, and Riess, Press, & Kirshner (1995), using Type Ia supernovae. These sparse, all-sky samples are suitable for measuring the convergence of the Local Group dipole motion to the cosmic microwave background dipole (or lack thereof), but they do not probe the velocity field on

scales of tens of megaparsecs. This requires the use of distance estimators that have greater precision per object or apply to clustered objects, allowing denser sampling.

FP-based distance estimators for elliptical galaxies fulfill these criteria. As recent work by Jørgensen et al. (1993) has shown, the FP can yield distances with errors as low as 11% per galaxy (compared to 17% for D_n - σ distances based on the same data and 25% for the original D_n - σ distances obtained by 7S). For individual *clusters*, it is possible to reduce the distance errors by $N^{1/2}$, where N is the number of galaxies in each cluster. With 5–15 elliptical galaxies per cluster it is therefore possible in principle to measure individual cluster distances with 3%–5% precision, corresponding to peculiar velocity errors of 500 – 750 km s^{-1} at a distance of $15,000 \text{ km s}^{-1}$. Thus, with sufficient clusters in a given volume, it becomes feasible to measure the peculiar velocity field with enough precision to reliably detect large-scale coherent motions at distances out to $15,000 \text{ km s}^{-1}$ that have amplitudes comparable to those observed in the local volume within 6000 km s^{-1} . Provided that significant sources of systematic error in the FP distance estimator can be ruled out or corrected for, the potential exists to determine the peculiar velocity fields in distant regions and thus further constrain cosmological models.

Two preparatory papers have discussed the photoelectric photometry and photometric system we use (Colless et al. 1993) and the methods we apply to correct for seeing in measuring the galaxies' light profiles (Saglia et al. 1993b), an important effect for galaxies at greater distances. Other aspects of this project and some preliminary results have been reported in Wegner et al. (1991), Davies et al. (1993), and Baggeley et al. (1993).

This paper (Paper I) describes how the galaxy clusters and galaxies belonging to those clusters were selected for this project. Future papers in this series will detail the spectroscopic and photometric data we have obtained, describe the methods used to analyze the luminosity profiles of the galaxies, examine the intrinsic properties of the galaxies and their dependence on environment, derive an optimal distance estimator, and discuss the peculiar motions of the galaxies and clusters and their significance for models of the large-scale structure of the universe.

In § 2 of this paper, we describe the selection of the regions and clusters used in this study, setting them in context with the surrounding large-scale structures. Section 3 gives the procedures used to select candidate elliptical galaxies in each cluster and gives the master list of basic information on the galaxies in the study. The selection functions for the galaxies in each cluster are quantified in § 4, and the conclusions we draw from this analysis are given in § 5.

2. SELECTION OF THE CLUSTER SAMPLE

We wanted to probe the peculiar velocity field of the galaxies to greater distances than had been sampled in the 7S study, in order to discover whether the motions found locally within 4000 km s^{-1} are typical of elsewhere in the universe. In order to achieve this, we chose two regions of similar size at sufficient distance from each other and the main parts of the Local Supercluster that their peculiar motions should be largely independent of the mass concentrations that produce bulk motions in the local volume. Choosing directions perpendicular to the supergalactic plane ensures the maximum separation between our two

regions and helps avoid possible confusion with distant parts of the Local Supercluster.

The depth of the sample is dictated by the choice of the distance indicator. For example, if a distance indicator has errors of $\sim 20\%$ for individual objects, then at $\sim 10,000 \text{ km s}^{-1}$, motions less than 1000 km s^{-1} can only be detected by averaging over several galaxies. The strong clustering of elliptical galaxies allows the selection of sets of galaxies at the same distance, so the fundamental plane for elliptical galaxies is a natural choice for the distance estimator. We have chosen our regions to lie in the range $cz = 6000\text{--}15,000 \text{ km s}^{-1}$ —from about twice the outer limit of the 7S sample to about the practical upper limit of the distance indicator.

An *all-sky* survey at this depth would have been considerably more difficult. As it was, ~ 350 galaxies had to be observed in each region to obtain sufficient sampling. Moreover, an all-sky survey is not necessary to achieve our goal of comparing the bulk motions of other regions with the local motions within a distance of $\sim 6000 \text{ km s}^{-1}$. We expect that the geometry of the sample is well suited for picking out specific components of the bulk flow if we compare, e.g., with Lauer & Postman (1994), though not as sensitive to all other directions (cf. Kaiser 1988; Feldman & Watkins 1994; Watkins & Feldman 1995).

These considerations led us to look for regions that were rich in clusters (so that they could be well sampled) and lie out of the supergalactic plane at distances between 6000 and $15,000 \text{ km s}^{-1}$. The selection of suitable regions and clusters (by which we mean elliptical-rich galaxy associations, ranging from Abell clusters to poor groups) was accomplished in two steps.

1. *Selection of the regions.*—Our cluster sample is based on the Abell (1958) catalog and Jackson's (1982) unpublished list of elliptical-rich groups and clusters. To select suitable regions, we compiled a list of all the Abell and Jackson clusters with redshifts in the range $cz = 6000\text{--}15,000 \text{ km s}^{-1}$ as given by Struble & Rood (1987) and Jackson (1982). Examining the distribution of these clusters on the sky led us to choose two regions, which we will refer to as HCB (Hercules–Corona Borealis) and PPC (Perseus–Pisces–Cetus), although they do *not* correspond precisely to the supercluster complexes with similar names identified by Tully & Fisher (1987). HCB is bounded by $\alpha = 13^{\text{h}}\text{--}19^{\text{h}}$ and $90^\circ > \delta > -21^\circ$ and PPC by $\alpha = 21^{\text{h}}\text{--}06^{\text{h}}$ and $90^\circ > \delta > -27^\circ$, in both cases excluding the region with $|b| < 10^\circ$. The declination limit in HCB is the southern limit of Jackson's catalog; in PPC we extended this limit to incorporate some more-southerly clusters at $\alpha \approx 5^{\text{h}}$.

Subsequent examination of the redshift distributions in each cluster showed that many have foreground or background galaxies or groups superposed on them. The problems caused by such contamination have been discussed in the literature (e.g., Primack et al. 1991) and will be dealt with in the context of our sample in a subsequent paper. Here we note that it complicates the problem of selecting a volume-limited sample of clusters. In particular, we find that the redshift of an Abell cluster given in the literature is sometimes that of a bright foreground galaxy while the true cluster is more distant (see below).

2. *Inspection of the Sky Survey plates.*—We next examined glass copies of all the Palomar Observatory Sky Survey (POSS) E plates in these two areas and the J plates from the SERC Sky Survey in the south, identifying the

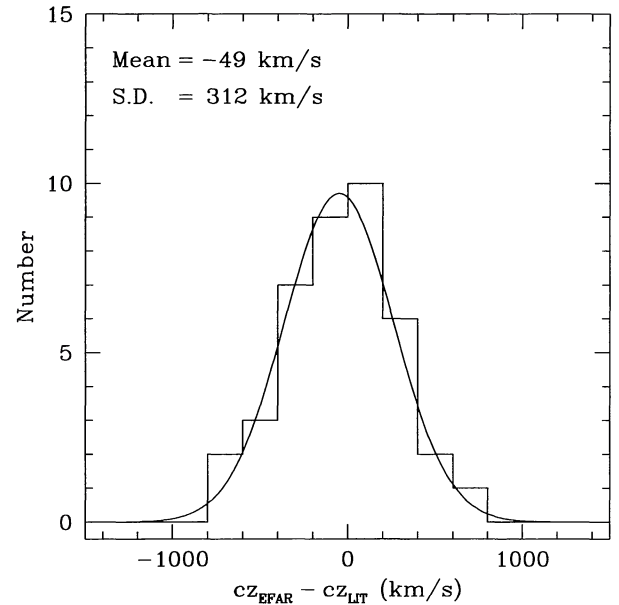


FIG. 1.—Distribution of differences between our median redshifts for each Abell cluster in our sample and the cluster redshifts given by NED. The curve is a Gaussian with mean and standard deviation determined from the data.

Abell and Jackson aggregates. In addition, we searched the plates to find all elliptical galaxies in each region with diameters (or redshifts, if they appeared in the Huchra redshift catalog) that indicated they were likely to be at roughly the same distance as the Struble & Rood (1987) and Jackson (1982) clusters on the plate. This led us to identify some aggregates not previously cataloged and, in a few cases, led us to follow the galaxy distributions onto neighboring Sky Survey plates. Only those aggregates that contained at least three elliptical galaxies, as judged by examining the plates, were retained for further study. The KPNO photographic lab then made enlargements of all the cluster fields found on the plates in order to provide a standard set of images that would allow us to select galaxies in a more reproducible way than is possible from the glass Sky Survey plates. The selection of the galaxy sample is described in detail in § 3.

Table 1 lists the clusters in our sample. The columns give, from left to right, the cluster ID number (CID), the number N of sample galaxies selected in the cluster, the right ascension and declination (J2000), the Galactic coordinates (l , b), the median redshift cz_{EFAR} in km s^{-1} (from the cluster members in our sample), the redshift from the literature cz_{lit} (obtained using NED²), and the name of the cluster. The cluster positions are in fact those of the “A” galaxy in the cluster (normally the brightest; see § 3), and so are not necessarily coincident with the Abell catalog positions. The table includes the 84 program clusters we initially selected (CID = 1–84) and the Coma Cluster (CID = 90), our primary reference cluster.

For the 40 cases for which there is a redshift in the literature, Figure 1 shows the distribution of differences between the median cluster redshifts we obtained and the literature values (the notes to Table 1 indicate the few cases where we preferred another literature redshift to the one adopted by

² NED, the NASA/IPAC Extragalactic Database, is operated for NASA by the Jet Propulsion Laboratory at Caltech.

TABLE 1
CLUSTER SAMPLE

CID	<i>N</i>	R.A.	decl.	<i>l</i> (deg)	<i>b</i> (deg)	<i>c</i> <i>z</i> _{EFAR} (km s ⁻¹)	<i>c</i> <i>z</i> _{lit} (km s ⁻¹)	Name
1	7	00 39.4	+06 44	117.57	-56.02	12082	12471	A76
2	5	00 41.8	-09 18	115.23	-72.04	16614	16680	A85 ^a
3	12	00 56.4	-01 15	125.80	-64.07	13140	13307	A119
4	6	01 02.0	+26 57	125.87	-35.86	14052	...	J3
5	5	00 58.8	+12 58	125.72	-49.85	12684	...	J4
6	7	01 09.3	+02 12	132.02	-60.34	13042	13130	A147 ^b
7	12	01 12.4	+15 44	130.33	-46.82	13150	13400	A160
8	9	01 13.0	-00 15	134.36	-61.61	13473	13427	A168
9	4	01 25.4	+01 44	140.13	-59.99	9603	9594	A189
10	9	01 20.9	-13 51	151.84	-75.04	15390	...	J30
11	6	01 25.1	+08 41	136.94	-53.26	14701	14584	A193
12	12	01 37.2	-09 11	156.21	-69.05	12298	...	J32
13	9	01 50.7	+33 04	137.00	-28.17	11035	10433	A260
14	10	01 52.7	+36 09	136.59	-25.09	5161	4827	A262
15	7	02 25.6	+36 57	143.10	-22.18	10726	...	J7
16	13	02 30.2	+23 09	150.69	-34.33	9425	...	J8
17	7	02 46.0	+36 54	147.11	-20.52	14550	14659	A376
18	7	02 49.7	+46 58	143.01	-11.22	8426	...	J9
19	2	02 55.7	-14 12	195.20	-58.30	9235	...	J33
20	9	02 56.5	+15 54	161.84	-37.33	9518	9743	A397
21	14	02 57.5	+05 58	170.28	-45.00	6804	7189	A400
22	3	03 08.3	-04 08	183.86	-50.08	8660	...	J28
23	12	03 08.2	-23 41	214.31	-59.00	20329	19936	A419
24	6	04 33.6	-13 15	209.59	-36.49	9691	9844	A496
25	10	04 45.1	-15 52	213.90	-34.95	10809	...	J34
26	3	04 52.7	+01 14	197.18	-25.49	8933	...	J10
27	6	04 58.8	-00 29	198.62	-24.50	4490	...	P597-1
28	5	04 54.8	-18 06	217.47	-33.61	9530	...	J35
29	7	04 51.3	-17 30	216.40	-34.19	9460	...	J34/35
30	4	04 59.7	-18 34	218.49	-32.70	12701	...	P777-1
31	8	05 02.9	-20 21	220.77	-32.62	8254	...	P777-2
32	10	05 05.2	-19 13	219.72	-31.71	16392	...	P777-3
33	8	05 04.0	-23 59	224.95	-33.54	12422	...	A533-1
34	9	05 01.6	-22 36	223.18	-33.65	14543	14150	A533
35	19	05 48.6	-25 28	230.28	-24.43	12357	12291	A548-1
36	17	05 42.3	-26 05	230.40	-25.97	11629	12291	A548-2
37	8	13 05.6	+53 33	118.21	63.43	8868	...	J11
38	8	13 43.4	+30 04	50.52	78.23	12685	...	J12
39	18	13 55.2	+25 03	28.27	75.54	8855	...	J13
40	7	14 08.1	-09 04	332.77	49.31	11437	...	J36
41	9	14 47.0	+13 40	12.21	59.85	9114	...	J14
42	10	14 47.1	+11 35	8.80	58.73	8806	...	J14-1
43	10	14 54.3	+16 21	18.59	59.60	13740	13238	A1983 ^c
44	11	14 54.5	+18 38	22.74	60.52	16845	17567	A1991 ^d
45	12	15 19.0	+04 31	6.81	48.20	10973	...	J16
46	11	15 11.6	+04 29	5.08	49.63	11129	...	J16W
47	3	15 21.9	+08 25	12.36	49.83	12850	...	A2063-S
48	10	15 12.8	+07 25	9.08	51.15	13544	13526	A2040
49	7	15 16.7	+07 01	9.42	50.11	10002	10432	A2052
50	10	15 23.0	+08 36	12.80	49.70	10381	10609	A2063
51	7	15 39.6	+21 46	34.41	51.51	12573	12369	A2107
52	10	15 55.0	+41 34	66.25	49.99	9988	...	J17
53	15	16 02.2	+15 58	28.91	44.53	10746	10537	A2147
54	4	15 57.1	+22 24	37.09	47.81	4430	...	P386-1
55	6	16 11.3	+23 57	40.53	45.09	9624	...	P386-2
56	9	16 03.3	+25 27	41.97	47.23	26322	26606 ^e	A2148
57	8	16 04.9	+23 55	39.95	46.50	9598	...	J18 ^f
58	16	16 04.5	+17 43	31.47	44.64	11122	11059	A2151
59	17	16 06.4	+15 41	29.06	43.50	13016	13047	A2152 ^g
60	8	15 58.3	+18 04	31.19	46.17	13890	...	P445-1
61	4	15 57.8	+16 18	28.77	45.63	10757	...	P445-2
62	6	16 13.2	+30 54	50.36	46.10	14866	...	A2162-N
63	11	16 12.5	+29 29	48.36	46.03	9668	9593	A2162-S ^h
64	5	16 18.0	+35 06	56.54	45.58	8960	...	J20
65	17	16 29.7	+40 48	64.68	43.50	9337	9134	A2197
66	19	16 28.6	+39 33	62.92	43.70	8892	9063	A2199
67	11	16 37.5	+50 20	77.51	41.64	13798	...	J21
68	8	16 52.8	+81 37	114.45	31.01	11559	11751	A2247
69	9	17 01.9	+28 25	49.95	35.22	10507	...	P332-1
70	8	16 57.9	+27 51	49.02	35.93	10394	...	J22 ⁱ
71	5	17 15.3	+57 24	85.81	35.40	8421	...	J23

TABLE 1—*Continued*

CID	<i>N</i>	R.A.	decl.	<i>l</i> (deg)	<i>b</i> (deg)	<i>cz</i> _{EFAR} (km s ⁻¹)	<i>cz</i> _{lit} (km s ⁻¹)	Name
72.....	6	17 33.0	+43 45	69.51	32.08	10383	...	J24
73.....	3	17 55.8	+62 36	91.82	30.22	8245	...	J25
74.....	5	18 02.6	+42 47	69.59	26.60	15083	...	J26
75.....	5	18 36.3	+51 27	80.41	23.15	9754	...	J27
76.....	4	21 41.0	-16 41	36.09	-44.90	15540	...	J38
77.....	12	22 50.0	+11 41	81.75	-41.26	7610	...	P522-1 ^j
78.....	7	23 18.7	+18 41	94.28	-38.95	11338	11841	A2572
79.....	10	23 23.9	+16 46	94.64	-41.23	12657	12621	A2589
80.....	18	23 24.3	+14 38	93.44	-43.19	12420	12981	A2593-N
81.....	7	23 24.4	+13 58	93.05	-43.79	12708	12981	A2593-S
82.....	13	23 38.5	+27 01	103.50	-33.08	9463	9354	A2634
83.....	9	23 44.9	+09 12	96.73	-50.25	12252	12099	A2657
84.....	5	23 50.9	+27 09	106.71	-33.80	8389	7945	A2666
90.....	32	12 59.6	+27 58	58.00	88.00	6769	6853	COMA ^k

NOTES.—Units of right ascension are hours and minutes, and units of declination are degrees and arcminutes (J2000). The Sky Survey fields originally examined for the cluster selection are (P = POSS, S = SERC): P010, P102, P103, P133, P141, P155, P179, P225, P226, P228, P229, P245, P246, P247, P273, P276, P294, P297, P324, P330, P332, P351, P354, P381, P385, P386, P403, P408, P412, P442, P445, P463, P467, P468, P502, P503, P522, P523, P526, P528, P532, P563, P584, P587, P588, P595, P597, P649, P653, P655, P680, P706, P708, P709, P712, P777, P819, S480, S486, S488.

^a CID = 2: A85 is also J29, the name used by Colless et al. 1993; *cz*_{lit} is from Fetisova 1982.

^b CID = 6: A147 was incorrectly called A150 in Colless et al. 1993.

^c CID = 43: A1983 was incorrectly called A1983-1 in Colless et al. 1993.

^d CID = 44: A1991 was incorrectly called A1983 in Colless et al. 1993.

^e CID = 56: A2148's *cz*_{lit} is from Postman & Lauer 1995.

^f CID = 57: J18 is also AWM 4.

^g CID = 59: A2152 is also J19, as used by Colless et al. 1993; *cz*_{lit} is for the brightest cluster galaxy (UGC 10187) from RC3.

^h CID = 63: A2162-S is A2162.

ⁱ CID = 70: J22 is also AWM 5.

^j CID = 77: P522-1 was incorrectly called A2506 in Colless et al. 1993.

^k CID = 90: COMA is A1656; *cz*_{lit} is from Colless & Dunn 1996.

NED). The scatter of 312 km s⁻¹ shown in Figure 1 is consistent with the 200–400 km s⁻¹ errors expected when estimating the mean redshift of clusters with line-of-sight velocity dispersions in the range 500–1000 km s⁻¹ from six galaxy redshifts (the median number of usable objects in our sample). The mean difference of -49 km s⁻¹ is consistent with the standard error in the mean expected from the observed scatter. Better estimates of the individual errors of the cluster *cz*_{EFAR} in Table 1 first require the assignment of membership to the clusters. That can only be finalized by using both redshift and distance information, because of the foreground and background objects. That information will be presented in subsequent papers dealing with the spectroscopy (Wegner et al. 1996) and the photometry (Saglia et al. 1996).

The cluster names given in Table 1 are either the Abell number (e.g., A2052) from the catalogs of Abell (1958) and Abell, Corwin, & Olowin (1989); Jackson numbers (e.g., J17) from Jackson (1982); or P-numbers, which combine the number of the Sky Survey field on which the cluster was found with a sequence number (e.g., P777-1, P777-2). Some clusters were split into suspected components (there is a J34/35 as well as J34 and J35, an A533-1 as well as A533, an A2162-N and an A2162-S, etc.). Some clusters have alternate names: A85 is also J29, A2152 is also J19, our A2162-S is A2162, and of course Coma is A1656. A few clusters were misnamed in Colless et al. (1993): A85, A147, A1983, A1991, A2152, and P522-1 were called J29, A150, A1983-1, A1983, J19, and A2506 in that paper; the names are given correctly in Table 1, and the galaxies in these clusters are also renamed in the list of sample galaxies (see § 3 and Table 3 below).

The locations of the survey regions and the 84 program clusters are shown in Figure 2. The projection in Galactic coordinates is shown for three redshift shells, with the middle shell corresponding to the nominal redshift range of our cluster sample, *cz* = 6000–15,000 km s⁻¹. In order to illustrate the level of completeness in our sample, the figure also shows the positions of all Abell clusters (Abell et al. 1989, excluding supplementary clusters) with measured redshifts (extracted from NED in 1995 May). Figure 2 also shows the direction of the Local Group's motion with respect to the cosmic microwave background (CMB) (Smoot et al. 1992) and with respect to the reference frame of Abell clusters within 15,000 km s⁻¹ (Lauer & Postman 1994; Colless 1995). The HCB and PPC regions are well away from the CMB dipole direction, while the Lauer & Postman dipole lies toward the edge of PPC.

A summary of the numbers of Abell (*N*_A), Jackson (*N*_J), and supplementary P-numbered (*N*_P) clusters and their sum (*N*_S) as a function of redshift range is given in Table 2 and shows that we were very successful in choosing clusters in the nominal redshift range 6000–15,000 km s⁻¹. Only 11 of the 84 program clusters are outside this range, and only two lie outside the range 4000–17,000 km s⁻¹. These two clusters are A419 (CID = 23, *cz* = 20,329 km s⁻¹) and A2148 (CID = 56, *cz* = 26,322 km s⁻¹). They were selected on the basis of redshifts from Struble & Rood's compilation (12,180 and 13,250 km s⁻¹, respectively) that proved erroneous. Note that Coma is not a program cluster; although it has an appropriate redshift, it lies just outside the survey region (it is the Abell cluster nearest the north Galactic pole in Fig. 2), and the galaxies in it were not selected in the same way (see below).

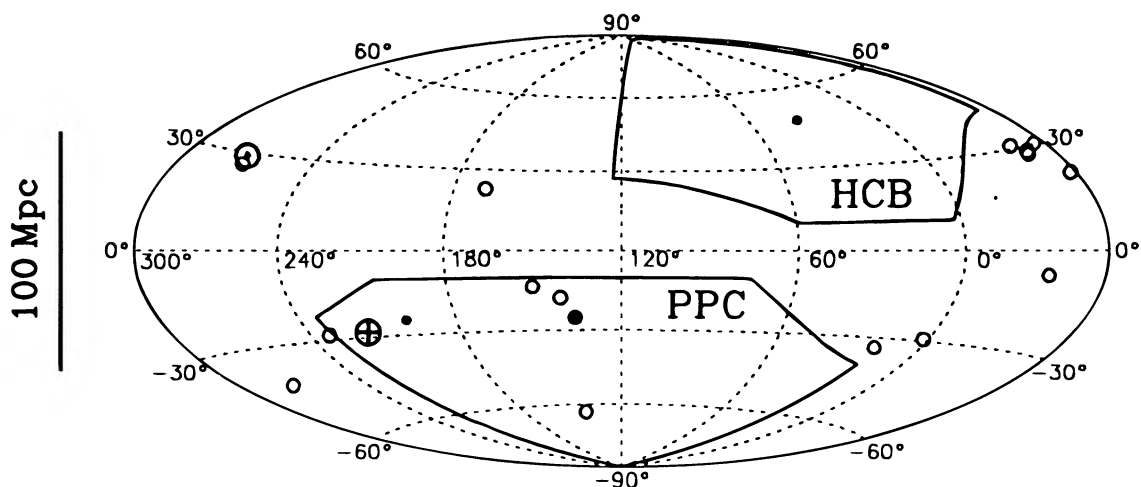


FIG. 2a

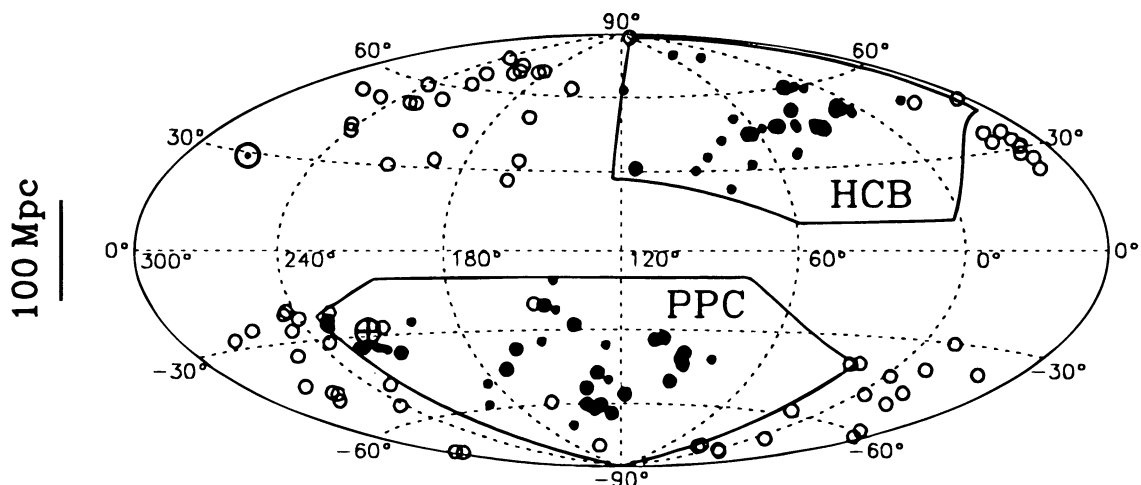


FIG. 2b

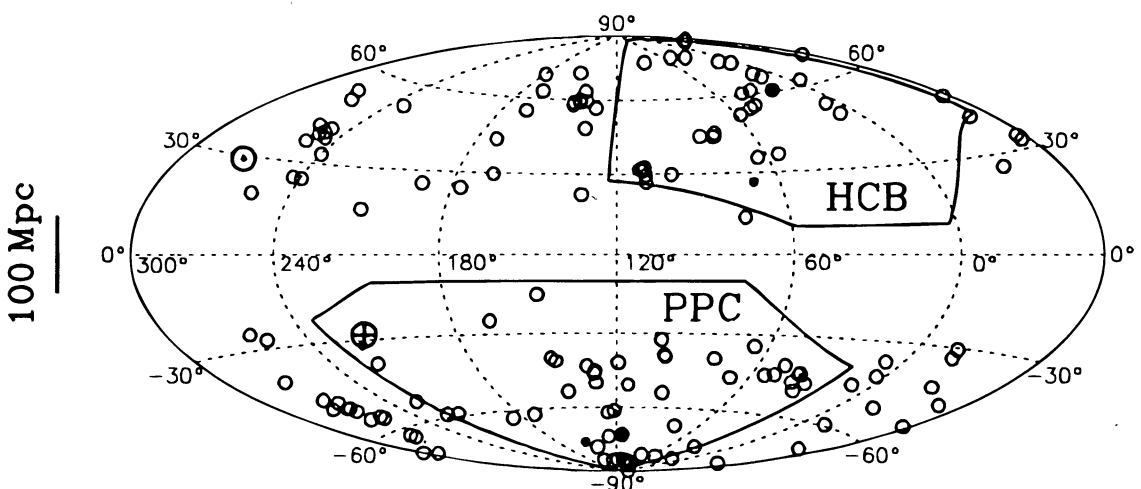


FIG. 2c

FIG. 2.—The EFAR cluster sample compared to the overall distribution of Abell clusters. The boundaries of the HCB and PPC regions on the sky are indicated. Large circles are Abell clusters (filled if they are in the EFAR sample); small dots are non-Abell clusters in the EFAR sample. The three panels show the cluster distribution (in an Aitoff projection of Galactic coordinates) for three redshift ranges: (a) $cz = 0\text{--}6000\text{ km s}^{-1}$; (b) $cz = 6000\text{--}15,000\text{ km s}^{-1}$; (c) $cz = 15,000\text{--}20,000\text{ km s}^{-1}$. The scale in $h^{-1}\text{ Mpc}$ at the upper end of each redshift range is indicated by the bar at left. Also indicated are the direction of the Local Group's motion with respect to the CMB (\odot) and with respect to the Lauer-Postman (1994) dipole for the Abell clusters within $15,000\text{ km s}^{-1}$ (\oplus).

TABLE 2
CLUSTER SAMPLE BY TYPE AND REDSHIFT

<i>cz</i> Range	N_A	N_J	N_P	N_S
HCB				
<6000	0	0	1	1
6000–15000	14	17	4	35
15000–20000	1	1	0	2
>20000	1	0	0	1
Total	16	18	5	39
PPC				
<6000	1	0	1	2
6000–15000	23	12	3	38
15000–20000	1	2	1	4
>20000	1	0	0	1
Total	26	14	5	45

In the nominal redshift range $cz = 6000\text{--}15,000 \text{ km s}^{-1}$, there are a total of 32 distinct Abell clusters in our sample, 12 in HCB and 20 in PPC. (The total of 37 in Table 2 arises because we split five Abell clusters into two components as a result of apparent substructure: A533, A548, A2063, A2162, and A2593.) NED lists a total of 50 Abell clusters in the survey region over this same redshift range, 15 in HCB and 35 in PPC (Abell et al. 1989, excluding supplements). However, scrutiny of the literature references and comparison with the Sky Survey plates provide strong evidence that the NED redshifts for a significant number of the Abell clusters that apparently should have been in our sample are incorrect, mostly belonging to foreground objects (see Appendix for details).

Excluding these clusters as very probably outside our sample redshift range, we find there are in fact 13 Abell clusters in the HCB volume and 27 in the PPC volume, so that our samples of Abell clusters are $12/13 \approx 92\%$ complete in HCB and $20/27 \approx 74\%$ complete in PPC. In fact, four of the clusters missed from our PPC sample are from Abell et al. (1989), which was not available when we were selecting our sample; excluding these, our completeness in PPC is $20/23 \approx 87\%$. The selection of our cluster sample will need to be accounted for in interpreting the results obtained on the velocity field.

The location of our survey volumes with respect to the major large-scale structures is illustrated in Figure 3, which shows the program clusters relative to the superclusters identified by Einasto et al. (1994). These are very similar to the superclusters given in the earlier supercluster catalogs of Bahcall & Soneira (1984), Batuski & Burns (1985), Tully & Fisher (1987), Tully et al. (1992), and Zucca et al. (1993), differing only in the effective density threshold used to define the superclusters and in having more Abell clusters with redshifts to work with. The names of the superclusters are those given in Einasto et al. (following earlier authors) except for Pisces A and Pisces B, which we have supplied for Einasto et al.'s superclusters 16 and 17. The volume we call HCB is centered on the Hercules supercluster at $10,000 \text{ km s}^{-1}$ and reaches toward (but does not encompass) the Corona Borealis and Bootes superclusters at $\sim 20,000 \text{ km s}^{-1}$. It does not include any other superclusters identified by Einasto et al. The PPC volume includes the Perseus-Pegasus A, Pisces A, and Lepus superclusters at distances of $\sim 12,000 \text{ km s}^{-1}$ and has an outer boundary that does not quite include the Pisces B, Pisces-Cetus, and Horologium-

Reticulum superclusters at $\sim 18,000 \text{ km s}^{-1}$.

3. SELECTION OF THE GALAXY SAMPLE

The search for suitable elliptical galaxies in each of the selected clusters was carried out using the high-quality enlargements of the relevant regions of Sky Survey glass copies described above. These enlargement prints greatly aided the uniform selection of our galaxy sample and the quantification of the selection criteria. Galaxies were selected entirely by their morphology and size on the enlargements. As redshifts were unavailable for many of the galaxies in our program clusters, we used the elliptical galaxies with known redshifts as a guide in finding other galaxies with elliptical morphologies and similar apparent sizes. We erred on the side of including some objects with disks rather than exclude possible elliptical galaxies. In order not to bias the selection, we did not identify known galaxies, but chose objects solely on the basis of their appearance on the Sky Survey enlargement prints.

From our previous experience (Faber et al. 1989), high-quality photographic enlargements of the Sky Survey glass copies can be used to make a quantifiable selection of elliptical galaxies. Thus an initial survey of the enlargements was conducted by picking out suitably sized objects that could possibly be E or S0 galaxies. As many galaxy images are saturated on the Sky Survey plates, we realized at the outset that this selection procedure also yields spiral galaxies, which would have to be weeded out with further imaging. However, we decided it was preferable to use an inclusive procedure in order to make the selection criteria more readily quantifiable and to bear the overhead of the extra subsequent imaging needed to make final morphological classifications.

All galaxies identified as possible E or S0 galaxies by the initial selection process were given capital-letter designations within each cluster (e.g., A119 A, J3 C, P777-3 B). This yielded 598 E/S0 galaxy candidates. A second pass through the selection process added 145 additional candidates (generally fainter, smaller galaxies), which were given numerical designations (e.g., A119 2, J3 1) to distinguish them from the first set. Altogether we selected a total of 743 E/S0 galaxy candidates in the program clusters. The final list of galaxies useful as distance indicators was further refined after spectroscopy and spectra were obtained.

In order to have a calibration and comparison sample, we also chose 52 well-studied galaxies in Coma, Virgo, and the field. These galaxies were *not* selected in the same way as the program galaxies but were drawn from samples studied by previous workers investigating the D_r - σ and FP relations. Our primary comparison sample of 32 Coma Cluster galaxies are designated by their Dressler (1984) numbers (e.g., COMA 124 is D124). The seven Virgo Cluster and 13 field galaxies are called by their NGC names (e.g., N4486 is NGC 4486).

Table 3 gives the basic data on all 795 objects observed in the EFAR project, listing the galaxy identification number (GIN), the galaxy's name, its position (J2000), the *R*-band extinction A_R , derived as described below, the Galactic coordinates (l , b), the logarithm of the photographic diameter D_w in arcseconds (see § 4), and some comments, which include other names for the galaxies (mainly NGC/IC names). The GIN is the unique identifier for each galaxy: the 743 program objects are assigned numbers 1–742 and 901 (P777-2 2). The 52 calibration galaxies are assigned

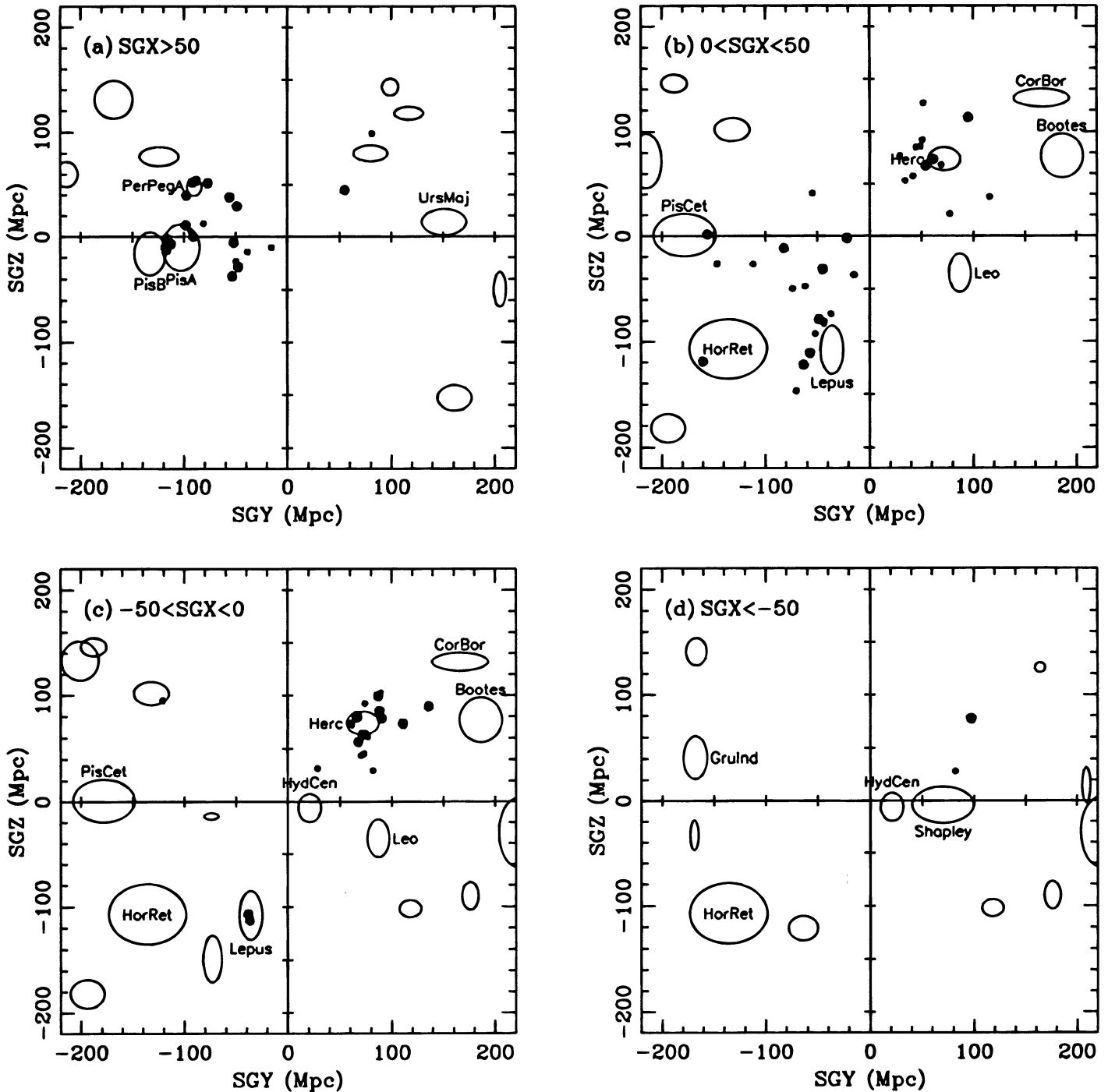


FIG. 3.—The EFAR cluster sample in relation to the surrounding large-scale structures. Large dots are Abell clusters and small dots are non-Abell clusters. The ellipses are the superclusters identified by Einasto et al. (1994), with the relevant ones named. The clusters and superclusters are shown projected onto the supergalactic SGY-SGZ plane, with the four panels corresponding to four slices in SGX: (a) $SGX > 50 \text{ h}^{-1} \text{ Mpc}$; (b) $0 < SGX < 50 \text{ h}^{-1} \text{ Mpc}$; (c) $-50 < SGX < 0 \text{ h}^{-1} \text{ Mpc}$; (d) $SGX < -50 \text{ h}^{-1} \text{ Mpc}$. The ellipses represent the size of each supercluster given by Einasto et al. (1994) and thus should correspond to their extent.

numbers 750–801. Note that there has been some renaming of the galaxies compared to Colless et al. (1993) because of the incorrect cluster names used in that paper. Only the cluster part of the name has been changed (following § 2 and the notes to Table 1); the alphanumeric designation (and the GIN) remains the same (e.g., A2506 A has become P522-1 A).

Of the total of 743 E/S0 galaxy candidates, it was subsequently found that there were three duplicated pairs (GINs $53 = 55$, $406 = 435$, $565 = 576$) and that four “galaxies”

are actually stars (GINs 123, 131, 133, 191); these are all noted in the comments column of Table 3. Excluding the duplicates and stars gives a sample of 736 galaxies that are E/S0 candidates. The distribution of the number of galaxies per program cluster is shown in Figure 4; the number of galaxies selected per cluster ranges from two to 19, with a median of eight.

Accurate positions were determined for all program galaxies by using the Galaxy Automated Scanning Program (GASP) of the Space Telescope Science Institute. The posi-

TABLE 3
MASTER LIST OF EFAR SAMPLE GALAXIES

GIN	Name		R.A.	decl.	A_R	l (deg)	b (deg)	$\log D_W$	Comments
1.....	A76	A	00 39 26.27	+06 44 03.3	0.037	117.60	-56.01	1.57	IC 1565
2.....	A76	B	00 40 28.02	+06 43 10.9	0.041	118.05	-56.05	1.36	IC 1569
3.....	A76	C	00 39 55.95	+06 50 55.0	0.037	117.83	-55.91	1.45	IC 1568
4.....	A76	D	00 40 30.59	+06 55 02.9	0.058	118.10	-55.85	1.49	
5.....	A76	E	00 38 54.76	+07 03 45.3	0.053	117.42	-55.67	1.36	NGC 0190
6.....	A76	F	00 39 04.56	+07 29 33.5	0.082	117.55	-55.25	1.41	
7.....	A76	1	00 40 44.71	+06 33 32.2	0.041	118.15	-56.21	1.23	
8.....	A85	A	00 41 50.40	-09 18 12.5	0.089	115.24	-72.03	1.54	Holmberg 015A, 015H
9.....	A85	B	00 41 50.07	-09 25 47.4	0.082	115.18	-72.16	1.10	
10.....	A85	C	00 42 54.67	-09 13 50.1	0.089	116.11	-71.99	1.24	
11.....	A85	1	00 43 10.15	-09 51 42.7	0.068	116.10	-72.62	1.24	
12.....	A85	2	00 41 22.23	-09 52 41.9	0.070	114.62	-72.59	1.20	
13.....	A119	A	00 56 25.63	-01 15 45.5	0.046	125.79	-64.11	1.39	
14.....	A119	B	00 56 16.09	-01 15 18.9	0.046	125.70	-64.10	1.65	
15.....	A119	C	00 57 34.95	-01 23 27.9	0.032	126.46	-64.22	1.45	3C 029
16.....	A119	D	00 56 56.98	-01 12 43.2	0.032	126.08	-64.05	1.31	
17.....	A119	E	00 56 02.67	-01 20 03.4	0.046	125.58	-64.18	1.26	
18.....	A119	F	00 55 40.64	-01 18 43.3	0.046	125.36	-64.16	1.35	
19.....	A119	G	00 55 18.82	-01 16 37.3	0.037	125.15	-64.13	1.15	
20.....	A119	H	00 57 45.27	-00 25 11.3	0.041	126.44	-63.25	1.54	
21.....	A119	I	00 57 27.84	-00 28 18.9	0.041	126.29	-63.30	1.31	
22.....	A119	J	00 57 17.12	-00 40 11.2	0.041	126.21	-63.50	1.31	
23.....	A119	1	00 56 12.82	-00 35 49.1	0.037	125.60	-63.44	1.09	
24.....	A119	2	00 55 21.46	-01 21 09.6	0.037	125.18	-64.21	1.26	
25.....	J3	A	01 02 05.44	+26 57 06.4	0.159	125.86	-35.86	1.50	
26.....	J3	B	00 58 47.45	+26 58 39.3	0.125	124.95	-35.87	1.28	
27.....	J3	C	00 59 24.44	+27 03 32.8	0.149	125.12	-35.78	1.24	IC 0064
28.....	J3	D	00 58 22.68	+26 51 58.7	0.125	124.84	-35.98	1.54	NGC 0326
29.....	J3	1	01 00 56.43	+27 09 53.1	0.154	125.53	-35.66	1.15	
30.....	J3	2	01 00 18.06	+26 56 57.3	0.149	125.37	-35.88	1.04	
31.....	J4	A	00 58 51.18	+12 58 21.2	0.085	125.73	-49.86	1.64	
32.....	J4	B	00 59 36.06	+12 59 09.7	0.073	126.02	-49.84	1.38	
33.....	J4	C	00 58 41.32	+12 41 35.0	0.099	125.69	-50.14	1.36	
34.....	J4	1	00 59 39.27	+12 57 34.1	0.073	126.04	-49.86	1.12	
35.....	J4	2	00 58 48.27	+13 05 57.5	0.085	125.71	-49.73	1.31	
36.....	A147	A	01 09 18.13	+02 12 15.1	0.010	131.98	-60.35	1.32	
37.....	A147	B	01 08 38.00	+02 16 06.5	0.008	131.63	-60.31	1.48	
38.....	A147	C	01 08 12.09	+02 11 37.5	0.008	131.43	-60.40	1.40	
39.....	A147	D	01 08 14.59	+02 10 36.1	0.008	131.46	-60.42	1.14	
40.....	A147	E	01 08 43.32	+02 11 31.0	0.008	131.70	-60.39	1.10	
41.....	A147	F	01 08 34.98	+02 09 44.2	0.008	131.63	-60.42	1.10	
42.....	A147	1	01 07 41.75	+02 07 09.2	0.010	131.20	-60.49	1.26	
43.....	A160	A	01 12 27.34	+15 44 59.9	0.053	130.33	-46.82	1.38	
44.....	A160	B	01 12 23.50	+15 43 33.8	0.053	130.31	-46.85	1.10	IC 1645
45.....	A160	C	01 10 28.96	+16 11 25.7	0.077	129.57	-46.44	1.30	
46.....	A160	D	01 12 18.66	+16 19 33.5	0.080	130.18	-46.25	1.23	
47.....	A160	E	01 13 15.75	+15 30 58.1	0.058	130.66	-47.03	1.53	
48.....	A160	F	01 13 02.89	+15 31 37.9	0.058	130.58	-47.02	1.35	
49.....	A160	G	01 12 59.67	+15 29 27.1	0.058	130.57	-47.06	1.51	
50.....	A160	H	01 13 47.70	+15 30 28.9	0.056	130.84	-47.02	1.19	
51.....	A160	I	01 11 24.88	+15 34 21.9	0.051	130.00	-47.02	1.23	
52.....	A160	J	01 14 14.44	+15 53 54.1	0.061	130.93	-46.62	1.57	
53.....	A160	1	01 11 50.18	+15 21 00.8	0.051	130.18	-47.23	1.05	Same as 55
54.....	A160	2	01 10 37.92	+16 14 42.8	0.063	129.62	-46.38	1.10	
55.....	A160	3	01 11 50.18	+15 21 00.8	0.051	130.18	-47.23	1.05	Same as 53
56.....	A168	A	01 13 00.07	-00 15 11.3	0.015	134.72	-62.63	1.64	NGC 0430
57.....	A168	B	01 12 48.76	-00 17 26.8	0.015	134.64	-62.68	1.52	NGC 0426
58.....	A168	C	01 14 21.60	+00 10 46.5	0.025	135.27	-62.14	1.32	
59.....	A168	D	01 14 57.64	+00 25 49.2	0.022	135.48	-61.87	1.42	
60.....	A168	E	01 14 54.38	+00 18 10.2	0.027	135.51	-61.99	1.15	
61.....	A168	F	01 15 15.83	+00 12 46.9	0.034	135.73	-62.07	1.24	
62.....	A168	G	01 16 12.86	-00 06 30.5	0.029	136.37	-62.33	1.15	
63.....	A168	1	01 15 16.88	+00 11 06.7	0.034	135.75	-62.09	1.20	
64.....	A168	2	01 14 46.35	-00 00 06.3	0.022	135.56	-62.30	1.32	
65.....	A189	A	01 25 31.36	+01 45 32.8	0.034	140.15	-59.97	1.96	NGC 0533
66.....	A189	B	01 24 47.80	+01 36 25.8	0.013	139.87	-60.16	1.49	IC 1694
67.....	A189	C	01 25 13.09	+02 03 58.4	0.041	139.84	-59.69	1.49	IC 0109
68.....	A189	D	01 24 36.50	+02 02 37.6	0.046	139.56	-59.75	1.53	IC 0103
69.....	J30	A	01 20 58.56	-13 51 00.8	0.008	151.84	-75.04	1.41	
70.....	J30	B	01 20 55.53	-13 50 06.2	0.008	151.77	-75.03	1.22	
71.....	J30	C	01 20 36.23	-13 51 50.0	0.008	151.55	-75.09	1.04	

TABLE 3—Continued

GIN	Name	R.A.	decl.	A_R	l (deg)	b (deg)	$\log D_W$	Comments
72	J30 D	01 20 34.24	−13 51 50.6	0.008	151.52	−75.09	1.22	
73	J30 E	01 20 20.61	−13 53 23.1	0.020	151.37	−75.14	1.27	
74	J30 F	01 20 20.53	−13 58 26.4	0.020	151.51	−75.22	0.97	
75	J30 G	01 19 16.79	−13 54 08.6	0.010	150.48	−75.26	1.17	
76	J30 1	01 20 04.97	−13 47 47.2	0.008	150.99	−75.09	1.11	
77	J30 2	01 19 32.19	−13 43 34.6	0.037	150.41	−75.08	1.27	
78	A193 A	01 25 07.66	+08 41 56.9	0.080	136.94	−53.25	1.50	IC 1695
79	A193 B	01 25 11.99	+08 39 20.1	0.080	136.98	−53.29	1.06	
80	A193 C	01 24 40.94	+08 36 31.5	0.065	136.79	−53.37	1.16	
81	A193 D	01 24 38.64	+08 30 35.0	0.080	136.81	−53.46	1.31	
82	A193 E	01 24 34.81	+08 34 34.2	0.065	136.76	−53.40	1.11	
83	A193 1	01 24 43.69	+08 46 33.4	0.065	136.75	−53.20	1.11	
84	J32 A	01 37 15.38	−09 11 51.7	0.053	156.19	−69.06	1.59	
85	J32 B	01 37 23.42	−09 10 07.9	0.065	156.23	−69.01	1.33	
86	J32 C	01 37 06.95	−09 08 58.0	0.053	156.04	−69.03	1.18	
87	J32 D	01 37 23.14	−09 16 14.5	0.053	156.37	−69.10	1.33	
88	J32 E	01 37 59.90	−09 00 26.6	0.065	156.37	−68.80	1.38	
89	J32 F	01 37 50.26	−08 58 50.4	0.065	156.24	−68.80	1.38	
90	J32 G	01 37 25.39	−08 55 53.7	0.056	155.93	−68.80	1.26	
91	J32 H	01 39 24.84	−09 24 04.0	0.049	157.76	−68.96	1.43	NGC 0640
92	J32 1	01 38 22.32	−08 58 32.7	0.049	156.55	−68.73	1.08	
93	J32 2	01 37 23.39	−09 05 59.2	0.065	156.14	−68.95	1.22	
94	J32 3	01 37 15.68	−09 01 33.1	0.056	155.96	−68.91	1.26	
95	J32 4	01 36 27.66	−09 28 44.1	0.056	156.10	−69.40	1.13	
96	A260 A	01 50 43.02	+33 04 54.4	0.097	137.00	−28.17	1.52	IC 1733
97	A260 B	01 50 51.78	+33 05 31.9	0.097	137.03	−28.15	1.34	
98	A260 C	01 51 23.66	+33 01 51.3	0.092	137.17	−28.18	1.40	
99	A260 D	01 51 21.37	+33 11 10.5	0.092	137.12	−28.03	1.15	
100	A260 E	01 49 13.02	+33 05 44.0	0.082	136.65	−28.23	1.27	
101	A260 F	01 50 15.59	+33 29 43.4	0.082	136.78	−27.79	1.40	
102	A260 G	01 51 45.53	+33 32 14.1	0.068	137.11	−27.67	1.34	
103	A260 H	01 52 24.98	+33 30 26.4	0.068	137.26	−27.66	1.19	
104	A260 1	01 50 32.13	+33 02 49.7	0.097	136.97	−28.21	1.23	
105	A262 A	01 52 46.45	+36 09 06.8	0.145	136.57	−25.09	1.87	NGC 0708
106	A262 B	01 50 51.29	+36 16 31.7	0.125	136.12	−25.07	1.68	
107	A262 C	01 50 33.28	+36 22 14.1	0.125	136.03	−24.99	1.74	NGC 0687
108	A262 D	01 49 43.79	+35 47 06.8	0.111	136.01	−25.60	1.68	NGC 0679
109	A262 E	01 55 10.27	+35 16 53.6	0.123	137.34	−25.80	1.79	IC 0171
110	A262 F	01 53 08.53	+36 49 10.8	0.121	136.46	−24.43	1.68	NGC 0712
111	A262 G	01 57 50.41	+36 20 34.3	0.123	137.60	−24.63	1.61	NGC 0759
112	A262 H	01 58 54.87	+36 40 28.9	0.121	137.72	−24.25	1.57	IC 0178
113	A262 I	01 52 39.68	+36 10 16.5	0.145	136.54	−25.08	1.68	NGC 0703
114	A262 1	01 54 53.95	+36 55 03.8	0.113	136.80	−24.24	1.53	A0151+36
115	J7 A	02 25 38.27	+36 57 51.3	0.142	143.10	−22.19	1.57	
116	J7 B	02 25 27.43	+37 10 26.7	0.116	142.98	−22.01	1.48	A0222+36
117	J7 C	02 23 56.01	+37 03 45.3	0.118	142.72	−22.23	1.37	
118	J7 D	02 26 27.62	+37 02 24.3	0.142	143.23	−22.06	1.21	
119	J7 E	02 26 14.63	+37 17 30.3	0.116	143.08	−21.84	1.27	
120	J7 F	02 26 12.24	+37 13 17.7	0.142	143.11	−21.91	1.21	
121	J7 G	02 26 09.82	+36 47 04.7	0.109	143.28	−22.32	1.18	
122	J8 A	02 30 16.42	+23 09 12.3	0.185	150.67	−34.34	1.28	
123	J8 B	02 30 10.54	+23 08 33.5	0.185	150.65	−34.36	...	Star
124	J8 C	02 29 54.43	+23 05 48.5	0.185	150.61	−34.43	1.37	
125	J8 D	02 29 49.91	+23 06 29.6	0.169	150.59	−34.43	1.47	
126	J8 E	02 29 14.08	+23 04 56.5	0.169	150.45	−34.51	1.50	IC 1803
127	J8 F	02 29 34.98	+22 56 34.3	0.185	150.62	−34.60	1.28	IC 1806
128	J8 G	02 30 31.04	+22 56 56.7	0.185	150.84	−34.50	1.28	IC 1807
129	J8 H	02 28 39.84	+23 00 43.3	0.169	150.35	−34.63	1.11	
130	J8 I	02 29 13.98	+22 57 57.7	0.169	150.51	−34.61	1.23	
131	J8 J	02 28 20.94	+23 01 42.0	0.197	150.26	−34.65	...	Star
132	J8 K	02 27 33.18	+23 03 35.2	0.197	150.04	−34.70	1.17	
133	J8 L	02 27 44.34	+23 01 42.4	0.197	150.11	−34.71	...	Star
134	J8 1	02 29 14.30	+22 50 22.0	0.169	150.59	−34.73	0.87	
135	A376 A	02 46 04.03	+36 54 17.8	0.123	147.10	−20.53	1.35	
136	A376 B	02 45 48.39	+36 51 12.3	0.123	147.08	−20.60	1.10	
137	A376 C	02 45 43.87	+36 51 16.1	0.123	147.06	−20.60	1.04	
138	A376 D	02 46 50.09	+36 58 43.5	0.159	147.21	−20.39	1.15	
139	A376 E	02 45 13.82	+36 41 40.5	0.123	147.05	−20.79	1.20	
140	A376 F	02 45 12.56	+36 42 42.9	0.123	147.03	−20.78	1.10	
141	A376 G	02 45 04.07	+36 42 34.8	0.123	147.01	−20.79	1.20	
142	J9 A	02 49 45.56	+46 58 33.3	0.526	143.02	−11.23	1.74	IC 0257
143	J9 B	02 49 40.40	+46 57 15.1	0.526	143.01	−11.26	1.18	

TABLE 3—Continued

GIN	Name	R.A.	decl.	A_R	l (deg)	b (deg)	$\log D_W$	Comments		
144.....	J9	C	02 51 01.00	+46 57 16.5	0.517	143.22	−11.15	1.68	IC 0260	
145.....	J9	D	02 50 12.86	+47 10 51.0	0.526	142.99	−11.01	1.51		
146.....	J9	E	02 52 16.90	+46 54 47.1	0.519	143.44	−11.09	1.35		
147.....	J9	F	02 48 59.87	+47 06 11.8	0.526	142.84	−11.17	1.18		
148.....	J9	G	02 48 10.87	+47 01 36.0	0.608	142.75	−11.30	1.30		
149.....	J33	A	02 55 44.28	−14 12 30.0	0.037	195.18	−58.31	1.66		
150.....	J33	B	02 55 48.39	−14 15 14.5	0.032	195.28	−58.31	1.09		
151.....	A397	A	02 56 32.92	+15 54 36.3	0.159	161.83	−37.34	1.23		
152.....	A397	B	02 56 28.85	+15 54 57.0	0.159	161.81	−37.34	1.50		
153.....	A397	C	02 56 27.92	+16 00 28.6	0.248	161.74	−37.27	1.23		
154.....	A397	D	02 57 04.64	+15 58 59.2	0.248	161.91	−37.20	1.20		
155.....	A397	E	02 56 32.53	+16 00 14.8	0.248	161.76	−37.26	1.29		
156.....	A397	F	02 57 23.63	+16 05 41.8	0.248	161.91	−37.07	1.26		
157.....	A397	G	02 57 37.59	+16 04 03.7	0.248	161.98	−37.06	1.39		
158.....	A397	H	02 57 57.55	+16 06 19.1	0.245	162.04	−36.98	1.17		
159.....	A397	I	02 57 08.06	+15 58 47.2	0.248	161.93	−37.20	1.17		
160.....	A400	A	02 57 33.72	+05 58 36.0	0.190	170.28	−44.99	1.47		
161.....	A400	B	02 55 19.94	+06 07 29.0	0.164	169.54	−45.24	1.30		
162.....	A400	C	02 55 14.90	+06 10 38.6	0.171	169.47	−45.21	1.30		
163.....	A400	D	02 58 14.27	+05 58 18.0	0.190	170.46	−44.88	1.25		
164.....	A400	E	02 58 21.03	+06 05 41.4	0.190	170.37	−44.77	1.44		
165.....	A400	F	02 58 37.77	+06 10 32.8	0.190	170.37	−44.67	1.53		
166.....	A400	G	02 58 54.29	+06 06 57.8	0.190	170.50	−44.67	1.20		
167.....	A400	H	02 59 16.14	+06 07 59.6	0.190	170.58	−44.59	1.30		
168.....	A400	I	02 58 29.75	+06 18 22.3	0.190	170.22	−44.59	1.55		
169.....	A400	J	02 58 24.62	+06 35 30.2	0.188	169.93	−44.39	1.64		
170.....	A400	K	02 59 52.37	+06 31 57.5	0.200	170.37	−44.19	1.50		
171.....	A400	L	02 57 41.61	+06 01 35.4	0.190	170.26	−44.93	1.71		
172.....	A400	1	03 00 08.67	+05 48 15.2	0.176	171.12	−44.69	1.44		
173.....	A400	2	02 59 59.92	+05 58 02.9	0.173	170.92	−44.60	1.30		
174.....	J28	A	03 08 20.06	−04 08 19.2	0.092	183.86	−50.07	1.57		
175.....	J28	B	03 07 44.60	−04 19 09.6	0.087	183.94	−50.30	1.34		
176.....	J28	C	03 08 03.25	−04 23 59.8	0.087	184.11	−50.29	1.42		
177.....	A419	A	03 08 15.97	−23 41 29.6	0.003	214.30	−59.01	1.43		
178.....	A419	B	03 08 10.82	−23 40 53.9	0.003	214.27	−59.02	1.17		
179.....	A419	C	03 08 15.85	−23 40 47.2	0.003	214.28	−59.00	1.09		
180.....	A419	D	03 08 28.07	−23 46 30.6	0.000	214.48	−58.98	0.99		
181.....	A419	E	03 08 33.26	−23 47 55.3	0.000	214.53	−58.97	1.23		
182.....	A419	F	03 08 21.63	−23 38 47.7	0.003	214.22	−58.97	1.20		
183.....	A419	G	03 08 20.24	−23 37 32.3	0.003	214.18	−58.97	1.34		
184.....	A419	H	03 08 16.33	−23 33 50.2	0.003	214.06	−58.97	1.29		
185.....	A419	I	03 08 48.58	−23 26 07.3	0.003	213.88	−58.82	1.17		
186.....	A419	J	03 09 20.17	−23 25 44.4	0.003	213.92	−58.70	1.20		
187.....	A419	1	03 08 03.44	−23 35 52.0	0.003	214.10	−59.03	0.99		
188.....	A419	2	03 07 50.76	−23 48 54.5	0.013	214.49	−59.13	1.13		
189.....	A496	A	04 33 37.80	−13 15 43.3	0.015	209.59	−36.49	1.62		
190.....	A496	B	04 34 10.46	−13 22 12.7	0.017	209.78	−36.41	1.27		
191.....	A496	C	04 34 39.37	−13 23 30.6	0.017	208.75	−35.90	...	Star	
192.....	A496	D	04 33 57.05	−13 27 45.7	0.017	209.85	−36.50	1.30		
193.....	A496	1	04 35 06.96	−13 23 39.2	0.041	209.92	−36.21	1.18		
194.....	A496	2	04 33 41.55	−13 10 13.1	0.020	209.49	−36.44	1.30	NGC 1650	
195.....	A496	3	04 33 32.12	−13 10 20.7	0.020	209.47	−36.47	1.13		
196.....	J34	A	04 45 11.53	−15 52 13.4	0.181	213.90	−34.94	1.70		
197.....	J34	B	04 45 21.72	−15 47 29.0	0.142	213.83	−34.88	1.17		
198.....	J34	C	04 45 35.11	−16 01 18.6	0.065	214.11	−34.91	1.22		
199.....	J34	D	04 45 31.16	−16 04 17.7	0.065	214.16	−34.95	1.17		
200.....	J34	E	04 43 45.39	−15 49 01.5	0.166	213.68	−35.24	1.36		
201.....	J34	F	04 47 51.82	−15 31 31.3	0.123	213.81	−34.22	1.43		
202.....	J34	1	04 47 13.48	−15 55 25.5	0.070	214.18	−34.51	1.22		
203.....	J34	2	04 46 55.95	−16 26 17.4	0.065	214.73	−34.77	1.28		
204.....	J34	3	04 46 51.88	−16 20 09.1	0.065	214.61	−34.75	1.17	IC 0393	
205.....	J34	4	04 46 37.84	−16 18 15.6	0.065	214.55	−34.79	1.22		
206.....	J10	A	04 52 49.27	+01 15 31.5	0.178	197.18	−25.48	1.61		
207.....	J10	B	04 52 57.66	+01 15 22.5	0.178	197.20	−25.45	1.31		
208.....	J10	C	04 53 28.79	+01 16 55.6	0.178	197.25	−25.33	1.27		
209.....	P597-1	A	04 58 54.68	−00 29 21.4	0.149	199.70	−25.06	1.88		NGC 1713
210.....	P597-1	B	04 58 44.03	−00 28 41.8	0.149	199.66	−25.09	1.58		NGC 1709
211.....	P597-1	C	04 58 33.27	−00 33 12.0	0.173	199.71	−25.17	1.44		
212.....	P597-1	D	04 58 31.50	−00 34 30.3	0.173	199.73	−25.18	1.48		
213.....	P597-1	E	04 58 38.51	−00 17 28.2	0.149	199.47	−25.02	1.48		
214.....	P597-1	1	04 59 43.03	−00 35 58.9	0.149	199.91	−24.94	1.18		
215.....	J35	A	04 54 52.26	−18 06 55.7	0.068	217.46	−33.62	1.89	E522G020	

TABLE 3—Continued

GIN	Name	R.A.	decl.	A_R	l (deg)	b (deg)	$\log D_W$	Comments
216.....	J35 B	04 57 04.52	−18 17 09.2	0.094	217.87	−33.19	1.41	
217.....	J35 C	04 56 53.65	−18 14 43.8	0.094	217.81	−33.22	1.41	
218.....	J35 D	04 55 23.18	−18 23 14.3	0.061	217.81	−33.60	1.41	
219.....	J35 E	04 57 17.76	−17 27 15.5	0.094	216.97	−32.84	1.29	
220.....	J35 1	04 53 55.35	−18 20 44.2	0.061	217.62	−33.91	1.29	
221.....	J34/35 A	04 51 20.62	−17 30 14.3	0.056	216.40	−34.18	1.45	A0449—17
222.....	J34/35 B	04 52 12.23	−17 24 30.7	0.051	216.39	−33.96	1.72	
223.....	J34/35 C	04 47 34.26	−17 20 51.6	0.051	215.83	−34.96	1.39	
224.....	J34/35 D	04 47 04.10	−17 20 58.1	0.053	215.78	−35.08	1.45	
225.....	J34/35 1	04 51 00.10	−17 19 55.0	0.061	216.17	−34.20	1.26	
226.....	J34/35 2	04 50 41.65	−16 45 03.9	0.070	215.49	−34.05	1.31	
227.....	J34/35 3	04 48 00.05	−16 39 51.8	0.053	215.10	−34.62	1.31	
228.....	P777-1 A	04 59 47.30	−18 34 51.9	0.097	218.47	−32.70	1.51	E552G044
229.....	P777-1 B	05 00 24.30	−18 51 58.2	0.099	218.85	−32.66	1.23	
230.....	P777-1 C	04 59 33.35	−18 12 18.1	0.109	218.03	−32.61	1.36	
231.....	P777-1 1	05 01 27.78	−18 18 33.2	0.116	218.34	−32.23	1.09	
232.....	P777-2 A	05 02 54.33	−20 21 59.7	0.037	220.77	−32.63	1.48	E552G057
233.....	P777-2 B	05 03 11.53	−20 19 01.4	0.037	220.74	−32.55	1.33	
234.....	P777-2 C	05 03 03.56	−20 16 32.4	0.039	220.68	−32.56	1.06	
235.....	P777-2 D	05 03 23.43	−20 18 42.0	0.039	220.75	−32.50	1.06	
236.....	P777-2 E	05 04 14.86	−20 06 59.4	0.037	220.61	−32.25	1.48	
237.....	P777-2 F	05 03 47.48	−20 00 06.2	0.037	220.44	−32.31	1.31	
238.....	P777-2 1	05 03 29.86	−20 27 25.0	0.037	220.92	−32.53	1.01	
901.....	P777-2 2	05 03 26.15	−20 02 30.2	0.037	220.45	−32.40	1.53	E552G059
239.....	P777-3 A	05 05 16.35	−19 13 06.6	0.053	219.72	−31.71	1.32	
240.....	P777-3 B	05 05 12.75	−19 08 35.8	0.053	219.63	−31.70	1.35	
241.....	P777-3 C	05 04 35.55	−19 16 11.5	0.053	219.71	−31.88	1.37	
242.....	P777-3 D	05 06 20.79	−19 28 01.6	0.041	220.10	−31.56	1.51	NGC 1780, E553G001
243.....	P777-3 E	05 04 22.36	−19 02 26.3	0.053	219.44	−31.85	1.30	
244.....	P777-3 F	05 04 43.59	−19 18 37.5	0.053	219.77	−31.86	1.09	
245.....	P777-3 G	05 04 35.63	−19 19 20.8	0.053	219.77	−31.90	1.24	
246.....	P777-3 H	05 03 54.39	−19 07 43.5	0.053	219.49	−31.98	1.35	
247.....	P777-3 1	05 05 34.94	−19 09 24.4	0.053	219.68	−31.62	1.14	
248.....	P777-3 2	05 04 58.94	−19 18 58.1	0.053	219.80	−31.81	1.30	
249.....	A533-1 A	05 04 01.44	−23 59 48.2	0.027	224.97	−33.55	1.59	E486G023
250.....	A533-1 B	05 03 57.88	−24 00 32.8	0.027	224.98	−33.57	1.18	
251.....	A533-1 C	05 03 50.66	−23 31 01.3	0.017	224.40	−33.45	1.48	
252.....	A533-1 D	05 05 36.41	−24 19 54.6	0.013	225.48	−33.31	1.41	
253.....	A533-1 E	05 01 35.38	−23 44 47.4	0.013	224.48	−34.01	1.18	
254.....	A533-1 F	05 01 07.97	−23 44 28.0	0.005	224.43	−34.11	1.41	
255.....	A533-1 G	05 01 11.54	−23 56 34.5	0.005	224.67	−34.15	1.38	
256.....	A533-1 H	05 05 39.92	−23 44 49.7	0.017	224.82	−33.12	1.29	
257.....	A533 A	05 01 36.10	−22 36 03.6	0.008	223.17	−33.65	1.41	
258.....	A533 B	05 01 08.32	−22 34 58.7	0.008	223.11	−33.75	1.41	
259.....	A533 C	05 01 06.68	−22 34 57.1	0.008	223.10	−33.75	1.15	
260.....	A533 D	05 00 18.34	−22 23 38.5	0.010	222.82	−33.87	1.48	
261.....	A533 E	05 00 31.02	−22 18 28.8	0.010	222.74	−33.79	1.21	
262.....	A533 F	05 02 28.48	−22 43 40.6	0.017	223.39	−33.50	1.21	
263.....	A533 G	05 01 31.49	−22 58 58.9	0.005	223.60	−33.79	1.27	
264.....	A533 H	05 01 45.72	−23 09 42.1	0.008	223.82	−33.79	1.27	
265.....	A533 1	05 03 44.24	−23 19 24.3	0.008	224.18	−33.41	1.37	
266.....	A548-1 A	05 48 38.47	−25 28 41.0	0.000	230.28	−24.43	1.61	E488G027
267.....	A548-1 B	05 48 43.20	−25 28 39.6	0.000	230.28	−24.41	1.55	
268.....	A548-1 C	05 47 34.77	−25 32 46.4	0.000	230.26	−24.68	1.48	
269.....	A548-1 D	05 47 25.23	−25 34 20.4	0.000	230.27	−24.72	1.53	E488G016
270.....	A548-1 E	05 46 55.52	−25 38 09.1	0.000	230.30	−24.85	1.59	E488G013
271.....	A548-1 F	05 47 47.55	−25 44 45.5	0.000	230.48	−24.70	1.45	
272.....	A548-1 G	05 47 43.24	−25 54 56.9	0.003	230.66	−24.77	1.43	
273.....	A548-1 H	05 49 21.79	−25 20 48.3	0.000	230.20	−24.23	1.65	E488G033
274.....	A548-1 I	05 47 26.62	−25 14 50.5	0.000	229.94	−24.60	1.40	E488G019, VV 180b
275.....	A548-1 J	05 47 24.70	−25 15 22.5	0.000	229.95	−24.61	1.20	E488G015, VV 180a
276.....	A548-1 K	05 48 33.28	−25 21 52.9	0.000	230.15	−24.41	1.20	
277.....	A548-1 L	05 49 59.06	−25 44 22.3	0.000	230.66	−24.23	1.36	
278.....	A548-1 M	05 50 02.72	−25 46 16.0	0.000	230.70	−24.23	1.40	
279.....	A548-1 N	05 45 22.15	−25 47 30.6	0.003	230.33	−25.23	1.61	E488G006
280.....	A548-1 O	05 45 05.02	−25 47 42.0	0.000	230.31	−25.29	1.36	
281.....	A548-1 P	05 49 13.16	−25 36 43.6	0.000	230.47	−24.35	1.29	
282.....	A548-1 Q	05 45 27.20	−25 53 53.9	0.010	230.45	−25.25	1.20	
283.....	A548-1 R	05 45 27.74	−25 55 07.8	0.010	230.49	−25.25	1.10	E488G009, VV 162c
284.....	A548-1 1	05 46 34.05	−25 22 52.7	0.000	230.00	−24.84	1.25	
285.....	A548-2 A	05 42 18.85	−26 05 53.5	0.000	230.40	−25.98	1.48	
286.....	A548-2 B	05 42 04.62	−26 07 20.5	0.000	230.41	−26.04	1.64	
287.....	A548-2 C	05 42 04.79	−26 08 42.4	0.000	230.43	−26.04	1.48	

TABLE 3—Continued

GIN	Name	R.A.	decl.	A_R	l (deg)	b (deg)	$\log D_w$	Comments
288.....	A548-2 D	05 42 07.27	−26 11 54.4	0.000	230.49	−26.05	1.50	
289.....	A548-2 E	05 41 25.55	−26 14 31.2	0.000	230.48	−26.21	1.30	
290.....	A548-2 F	05 41 20.59	−26 15 34.5	0.000	230.49	−26.24	1.40	
291.....	A548-2 G	05 41 02.52	−26 11 14.0	0.000	230.39	−26.28	1.30	
292.....	A548-2 H	05 43 14.95	−25 54 12.5	0.049	230.27	−25.71	1.37	
293.....	A548-2 I	05 42 20.92	−25 32 29.0	0.022	229.82	−25.79	1.67	E487G036
294.....	A548-2 J	05 42 14.62	−25 32 25.4	0.022	229.81	−25.81	1.40	
295.....	A548-2 K	05 44 56.19	−25 55 16.8	0.049	230.43	−25.36	1.40	
296.....	A548-2 L	05 45 07.99	−26 05 35.1	0.000	230.63	−25.38	1.37	
297.....	A548-2 M	05 43 03.54	−25 59 07.3	0.000	230.34	−25.78	1.26	
298.....	A548-2 N	05 44 29.72	−26 03 32.6	0.000	230.54	−25.50	1.48	
299.....	A548-2 O	05 44 26.08	−26 04 41.4	0.000	230.55	−25.52	1.30	
300.....	A548-2 1	05 42 54.82	−26 18 43.9	0.000	230.68	−25.92	1.33	
301.....	A548-2 2	05 41 46.38	−25 51 57.5	0.015	230.11	−26.02	1.48	
302.....	J11 A	13 05 36.58	+53 33 49.9	0.020	118.22	+63.43	1.44	NGC 4967
303.....	J11 B	13 05 56.16	+53 39 32.8	0.020	118.14	+63.33	1.51	NGC 4973
304.....	J11 C	13 05 32.28	+53 41 05.6	0.020	118.28	+63.32	1.44	IC 0847
305.....	J11 D	13 05 03.09	+53 39 13.5	0.020	118.43	+63.36	1.44	
306.....	J11 E	13 05 25.93	+53 35 29.2	0.020	118.29	+63.41	1.24	
307.....	J11 F	13 07 21.93	+53 35 10.9	0.027	117.65	+63.38	1.47	
308.....	J11 1	13 06 50.97	+53 32 48.1	0.037	117.81	+63.43	1.16	
309.....	J11 2	13 06 25.02	+53 29 03.5	0.037	117.94	+63.50	1.16	
310.....	J12 A	13 43 24.96	+30 04 08.8	0.000	50.45	+78.23	1.35	NGC 5282
311.....	J12 B	13 42 55.61	+29 52 05.6	0.000	49.57	+78.37	1.38	NGC 5280
312.....	J12 C	13 42 48.71	+29 42 19.2	0.000	48.80	+78.42	1.28	
313.....	J12 D	13 44 14.21	+29 48 13.4	0.000	49.02	+78.10	1.28	
314.....	J12 E	13 42 23.39	+29 50 50.6	0.000	49.58	+78.49	1.35	NGC 5274
315.....	J12 F	13 42 23.64	+29 49 28.0	0.000	49.46	+78.49	1.35	
316.....	J12 1	13 44 11.74	+29 34 59.2	0.000	47.97	+78.14	1.24	
317.....	J12 2	13 41 17.06	+29 50 03.4	0.000	49.74	+78.72	1.10	
318.....	J13 A	13 55 13.46	+25 03 04.7	0.000	28.26	+75.54	1.52	IC 4345
319.....	J13 B	13 55 12.60	+25 01 15.2	0.000	28.14	+75.54	1.59	IC 4344
320.....	J13 C	13 55 34.47	+25 02 58.1	0.000	28.32	+75.46	1.38	Hickson 69B
321.....	J13 D	13 54 55.88	+25 07 20.3	0.000	28.48	+75.62	1.48	IC 4343
322.....	J13 E	13 53 40.70	+25 04 43.8	0.000	28.08	+75.89	1.43	
323.....	J13 F	13 52 44.93	+25 02 22.4	0.000	27.74	+76.09	1.38	
324.....	J13 G	13 52 37.52	+24 44 54.1	0.000	26.54	+76.05	1.59	
325.....	J13 H	13 51 05.48	+25 05 35.4	0.000	27.64	+76.46	1.48	
326.....	J13 I	13 51 04.69	+25 04 57.2	0.000	27.59	+76.46	1.08	
327.....	J13 J	13 50 31.88	+24 58 22.5	0.000	27.02	+76.56	1.38	Holmberg 546A
328.....	J13 K	13 50 30.87	+24 57 44.7	0.000	26.97	+76.56	1.33	Holmberg 546B
329.....	J13 L	13 50 25.15	+24 54 30.3	0.000	26.72	+76.57	1.08	
330.....	J13 M	13 49 52.58	+25 11 25.7	0.000	27.81	+76.75	1.33	IC 4332
331.....	J13 N	13 55 48.41	+24 48 17.8	0.000	27.41	+75.36	1.26	
332.....	J13 O	13 55 56.21	+24 57 02.2	0.000	28.00	+75.36	1.26	
333.....	J13 P	13 56 09.37	+25 11 42.5	0.000	28.99	+75.36	1.26	
334.....	J13 1	13 56 01.99	+24 40 30.7	0.000	26.96	+75.28	1.18	
335.....	J13 2	13 51 39.37	+24 41 17.4	0.000	26.08	+76.25	1.18	
336.....	J36 A	14 08 07.00	−09 04 18.4	0.039	332.76	+49.31	1.39	
337.....	J36 B	14 08 07.56	−09 03 42.8	0.039	332.77	+49.32	0.94	
338.....	J36 C	14 08 06.20	−09 04 41.5	0.039	332.75	+49.30	0.99	
339.....	J36 D	14 06 36.63	−09 13 45.6	0.032	332.14	+49.33	1.17	
340.....	J36 1	14 09 55.79	−09 04 55.7	0.037	333.36	+49.10	0.94	
341.....	J36 2	14 09 54.01	−08 49 22.2	0.037	333.53	+49.33	1.09	
342.....	J36 3	14 08 04.25	−09 09 09.6	0.039	332.68	+49.24	1.09	
343.....	J14 A	14 47 02.19	+13 40 04.3	0.010	12.22	+59.86	1.36	NGC 5758
344.....	J14 B	14 46 39.21	+13 40 32.6	0.010	12.13	+59.95	1.25	
345.....	J14 C	14 46 47.82	+13 41 40.3	0.010	12.20	+59.93	1.14	
346.....	J14 D	14 46 54.17	+13 42 35.8	0.010	12.25	+59.91	1.01	
347.....	J14 1	14 48 17.28	+13 45 25.1	0.010	12.68	+59.65	1.06	
348.....	J14 2	14 48 05.20	+13 28 48.9	0.010	12.16	+59.55	1.18	
349.....	J14 3	14 47 45.66	+13 20 31.6	0.005	11.84	+59.54	1.06	
350.....	J14 4	14 46 50.42	+13 50 51.8	0.010	12.47	+60.00	1.33	
351.....	J14 5	14 46 22.02	+13 28 35.6	0.005	11.72	+59.90	0.88	
352.....	J14-1 A	14 47 06.34	+11 35 36.9	0.013	8.81	+58.73	1.50	
353.....	J14-1 B	14 46 53.77	+11 37 33.7	0.013	8.80	+58.80	1.31	
354.....	J14-1 C	14 46 46.51	+11 34 11.5	0.015	8.68	+58.79	1.35	
355.....	J14-1 D	14 46 27.74	+11 30 24.9	0.015	8.50	+58.82	1.31	
356.....	J14-1 E	14 47 06.93	+10 59 57.6	0.015	7.87	+58.40	1.43	
357.....	J14-1 F	14 49 07.62	+10 58 46.2	0.008	8.37	+57.98	1.35	
358.....	J14-1 1	14 49 34.94	+11 14 52.6	0.005	8.91	+58.04	1.28	
359.....	J14-1 2	14 48 36.62	+11 19 31.4	0.005	8.78	+58.28	1.28	
360.....	J14-1 3	14 47 17.71	+11 07 47.9	0.015	8.12	+58.43	1.28	

TABLE 3—Continued

GIN	Name	R.A.	decl.	A_R	l (deg)	b (deg)	$\log D_W$	Comments
361.....	J14-1 4	14 46 53.56	+11 22 46.3	0.015	8.41	+58.66	1.20	
362.....	A1983 A	14 54 23.50	+16 21 17.6	0.010	18.58	+59.59	1.76	IC 4516
363.....	A1983 B	14 52 55.36	+16 42 09.4	0.010	18.90	+60.06	1.57	
364.....	A1983 C	14 52 56.91	+16 43 39.0	0.010	18.95	+60.06	1.43	
365.....	A1983 D	14 52 43.31	+16 54 12.6	0.015	19.22	+60.19	1.53	
366.....	A1983 E	14 52 22.90	+17 07 16.7	0.008	19.55	+60.35	1.53	
367.....	A1983 F	14 49 59.15	+16 48 35.6	0.008	18.48	+60.74	1.34	
368.....	A1983 G	14 49 56.99	+16 48 30.5	0.008	18.47	+60.74	1.23	
369.....	A1983 1	14 52 57.84	+16 41 48.3	0.010	18.90	+60.04	1.23	
370.....	A1983 2	14 51 14.66	+16 41 42.0	0.000	18.54	+60.41	1.34	
371.....	A1983 3	14 49 22.41	+16 25 55.8	0.003	17.65	+60.70	1.18	
372.....	A1991 A	14 54 31.54	+18 38 32.0	0.015	22.79	+60.50	1.66	NGC 5778
373.....	A1991 B	14 54 48.00	+18 33 49.3	0.015	22.69	+60.41	1.51	
374.....	A1991 C	14 54 17.98	+18 33 10.8	0.015	22.58	+60.51	1.42	
375.....	A1991 D	14 51 14.31	+18 45 25.9	0.022	22.40	+61.26	1.21	
376.....	A1991 E	14 51 17.70	+18 41 12.4	0.022	22.27	+61.22	1.49	IC 1062
377.....	A1991 F	14 53 40.02	+18 04 11.1	0.013	21.56	+60.46	1.29	
378.....	A1991 1	14 54 54.07	+18 50 11.5	0.020	23.22	+60.49	1.21	
379.....	A1991 2	14 54 05.16	+18 26 00.2	0.015	22.31	+60.51	1.21	
380.....	A1991 3	14 55 56.80	+18 02 48.9	0.025	21.95	+59.95	1.29	
381.....	A1991 4	14 55 58.08	+18 30 07.9	0.015	22.79	+60.13	1.17	
382.....	A1991 5	14 55 23.88	+18 50 08.1	0.020	23.31	+60.38	1.29	
383.....	J16 A	15 19 01.53	+04 31 13.5	0.039	6.82	+48.20	1.53	
384.....	J16 B	15 19 03.56	+04 19 59.6	0.027	6.60	+48.08	1.40	
385.....	J16 C	15 18 27.88	+04 40 30.6	0.039	6.88	+48.40	1.19	
386.....	J16 D	15 21 22.60	+04 20 28.9	0.027	7.13	+47.62	1.27	
387.....	J16 E	15 17 23.00	+04 12 47.8	0.022	6.08	+48.34	1.27	
388.....	J16 F	15 19 24.75	+04 34 45.5	0.039	6.98	+48.16	1.19	
389.....	J16 G	15 18 52.61	+04 51 55.6	0.041	7.20	+48.43	1.34	
390.....	J16 1	15 20 51.87	+04 23 27.5	0.027	7.07	+47.75	1.04	
391.....	J16 2	15 19 37.41	+04 26 53.7	0.027	6.87	+48.04	1.10	
392.....	J16 3	15 19 33.78	+04 20 15.3	0.027	6.72	+47.98	1.10	
393.....	J16 4	15 19 27.82	+04 05 44.2	0.025	6.41	+47.86	1.19	
394.....	J16 5	15 18 09.29	+04 33 45.6	0.039	6.67	+48.40	1.27	
395.....	J16W A	15 11 41.53	+04 29 26.9	0.051	5.10	+49.64	1.33	
396.....	J16W B	15 11 31.53	+04 31 01.5	0.049	5.09	+49.68	1.36	
397.....	J16W C	15 11 37.04	+04 28 01.6	0.049	5.05	+49.64	1.19	
398.....	J16W D	15 12 52.96	+04 30 48.4	0.053	5.41	+49.41	1.42	
399.....	J16W E	15 13 10.47	+04 28 54.2	0.053	5.43	+49.34	1.27	
400.....	J16W F	15 13 18.61	+04 28 37.4	0.053	5.46	+49.31	1.27	
401.....	J16W G	15 14 06.19	+04 13 18.0	0.027	5.34	+49.00	1.33	
402.....	J16W H	15 13 50.80	+04 37 19.4	0.032	5.76	+49.29	1.09	
403.....	J16W I	15 13 49.70	+04 43 23.2	0.058	5.88	+49.36	1.27	
404.....	J16W 1	15 13 43.46	+04 21 43.1	0.029	5.42	+49.16	1.09	
405.....	J16W 2	15 10 52.32	+04 52 03.8	0.058	5.37	+50.03	1.09	
406.....	A2063-S A	15 21 55.39	+08 25 24.5	0.049	12.34	+49.83	1.54	Same as 435, IC 1116
407.....	A2063-S B	15 20 53.32	+08 23 47.1	0.044	12.09	+50.03	1.37	
408.....	A2063-S C	15 21 36.91	+07 43 08.4	0.044	11.36	+49.51	1.26	
409.....	A2040 A	15 12 50.76	+07 25 25.5	0.032	9.07	+51.14	1.01	
410.....	A2040 B	15 12 47.60	+07 26 02.2	0.032	9.07	+51.16	1.26	
411.....	A2040 C	15 12 43.37	+07 26 48.1	0.032	9.07	+51.18	1.09	
412.....	A2040 D	15 12 37.66	+07 27 04.1	0.032	9.06	+51.20	1.01	
413.....	A2040 E	15 12 34.39	+07 25 51.9	0.032	9.02	+51.20	1.15	
414.....	A2040 F	15 11 31.44	+07 15 05.5	0.029	8.54	+51.31	1.31	
415.....	A2040 G	15 10 11.06	+07 37 41.8	0.029	8.73	+51.80	1.15	
416.....	A2040 H	15 09 28.27	+07 33 22.4	0.029	8.47	+51.90	1.21	
417.....	A2040 1	15 12 28.21	+07 58 24.0	0.025	9.71	+51.53	1.09	
418.....	A2040 2	15 11 16.11	+07 29 19.9	0.034	8.80	+51.50	1.15	
419.....	A2052 A	15 16 44.56	+07 01 15.6	0.027	9.42	+50.12	1.70	A1514+07
420.....	A2052 B	15 16 45.87	+07 00 14.6	0.027	9.40	+50.11	1.34	
421.....	A2052 C	15 16 53.98	+06 56 20.3	0.027	9.35	+50.04	1.16	
422.....	A2052 D	15 16 09.85	+06 57 51.3	0.025	9.22	+50.21	1.06	
423.....	A2052 E	15 16 09.99	+06 57 04.2	0.025	9.20	+50.20	1.06	
424.....	A2052 F	15 17 12.64	+07 01 40.9	0.027	9.53	+50.03	1.24	
425.....	A2052 G	15 17 10.91	+06 56 29.3	0.027	9.41	+49.98	1.06	
426.....	A2063 A	15 23 05.35	+08 36 31.9	0.044	12.82	+49.68	1.55	
427.....	A2063 B	15 23 10.92	+08 38 02.1	0.044	12.87	+49.68	1.13	
428.....	A2063 C	15 23 14.06	+08 38 42.3	0.044	12.90	+49.67	1.13	
429.....	A2063 D	15 23 15.06	+08 34 24.4	0.044	12.81	+49.63	1.25	
430.....	A2063 E	15 23 07.52	+08 31 41.0	0.044	12.72	+49.63	1.25	
431.....	A2063 F	15 23 10.45	+08 30 18.7	0.044	12.70	+49.61	1.13	
432.....	A2063 G	15 23 35.30	+09 20 45.1	0.046	13.89	+49.97	1.35	
433.....	A2063 H	15 23 39.26	+08 45 31.6	0.039	13.13	+49.65	1.25	

TABLE 3—Continued

GIN	Name	R.A.	decl.	A_R	l (deg)	b (deg)	$\log D_W$	Comments
434.....	A2063 1	15 24 37.34	+08 59 24.3	0.046	13.63	+49.57	1.19	
435.....	A2063 2	15 21 55.40	+08 25 24.6	0.049	12.34	+49.83	1.50	Same as 406, IC 1116
436.....	A2107 A	15 39 39.10	+21 46 56.3	0.109	34.39	+51.52	1.54	
437.....	A2107 B	15 39 22.96	+21 44 20.0	0.109	34.30	+51.57	1.24	
438.....	A2107 C	15 37 26.16	+21 44 36.5	0.101	34.09	+52.00	1.21	
439.....	A2107 D	15 39 56.82	+21 49 25.6	0.109	34.49	+51.47	1.16	
440.....	A2107 E	15 40 17.34	+21 54 52.9	0.113	34.66	+51.42	1.07	
441.....	A2107 1	15 40 46.69	+21 46 20.0	0.109	34.50	+51.27	0.94	
442.....	A2107 2	15 39 51.38	+21 42 13.6	0.109	34.29	+51.45	0.77	
443.....	J17 A	15 55 02.01	+41 34 40.7	0.017	66.26	+49.99	1.51	
444.....	J17 B	15 55 13.93	+41 34 53.5	0.017	66.26	+49.95	1.26	
445.....	J17 C	15 55 40.26	+41 30 16.1	0.010	66.13	+49.88	1.33	
446.....	J17 D	15 53 28.98	+41 34 47.9	0.025	66.31	+50.28	1.41	
447.....	J17 E	15 55 27.12	+41 33 29.0	0.017	66.22	+49.91	1.29	
448.....	J17 F	15 54 14.24	+41 24 52.9	0.017	66.03	+50.16	1.19	
449.....	J17 G	15 53 45.57	+41 23 23.7	0.017	66.01	+50.25	1.29	
450.....	J17 1	15 55 14.23	+41 28 00.8	0.017	66.08	+49.96	1.05	
451.....	J17 2	15 55 09.60	+41 26 54.2	0.017	66.06	+49.98	1.19	
452.....	J17 3	15 53 52.95	+41 29 50.9	0.017	66.17	+50.21	1.05	
453.....	A2147 A	16 02 17.10	+15 58 27.1	0.017	28.91	+44.52	1.76	A1600+16C, VV 159a, Arp 324
454.....	A2147 B	16 02 12.87	+15 54 26.2	0.017	28.81	+44.51	1.56	A1600+16A, VV 159c, Arp 324
455.....	A2147 C	16 02 19.92	+16 20 43.9	0.022	29.40	+44.65	1.58	
456.....	A2147 D	16 02 18.07	+16 21 56.4	0.017	29.42	+44.67	1.43	
457.....	A2147 E	16 03 14.80	+16 24 09.1	0.017	29.59	+44.47	1.51	
458.....	A2147 F	16 00 35.80	+15 41 07.4	0.029	28.31	+44.79	1.51	IC 1155
459.....	A2147 G	16 01 16.90	+15 38 41.8	0.029	28.35	+44.62	1.36	IC 1161
460.....	A2147 H	16 01 30.60	+15 30 12.6	0.029	28.20	+44.51	1.43	IC 1163
461.....	A2147 I	16 03 43.78	+16 19 38.2	0.017	29.55	+44.34	1.40	
462.....	A2147 J	16 03 45.91	+16 20 16.3	0.017	29.57	+44.33	1.13	
463.....	A2147 1	16 03 38.19	+15 54 01.7	0.029	28.99	+44.20	1.13	
464.....	A2147 2	16 02 40.43	+15 45 20.2	0.032	28.68	+44.35	1.36	
465.....	A2147 3	16 02 08.11	+15 41 46.8	0.032	28.53	+44.45	1.46	VV 090a, 090b
466.....	A2147 4	16 01 54.96	+16 27 15.3	0.017	29.48	+44.79	1.40	
467.....	A2147 5	16 01 21.26	+16 40 34.5	0.017	29.70	+45.00	1.40	
468.....	P386-1 A	15 57 08.24	+22 24 14.8	0.068	37.08	+47.81	1.71	NGC 6020, IC 1148
469.....	P386-1 B	15 58 17.52	+22 40 28.0	0.061	37.58	+47.63	1.42	
470.....	P386-1 C	15 58 06.96	+22 39 51.9	0.061	37.55	+47.67	1.06	
471.....	P386-1 1	15 58 12.49	+22 29 19.4	0.065	37.31	+47.60	1.06	
472.....	P386-2 A	16 11 22.62	+23 57 53.2	0.082	40.55	+45.08	1.51	NGC 6075, VV 380
473.....	P386-2 B	16 12 05.95	+23 50 28.8	0.082	40.44	+44.89	1.21	
474.....	P386-2 C	16 12 07.80	+23 43 04.6	0.082	40.27	+44.85	1.29	
475.....	P386-2 D	16 11 18.91	+24 10 54.0	0.101	40.84	+45.15	1.14	
476.....	P386-2 1	16 12 22.40	+24 12 25.0	0.092	40.96	+44.93	1.06	
477.....	P386-2 2	16 10 30.59	+24 03 14.5	0.106	40.60	+45.30	1.17	
478.....	A2148 A	16 03 19.91	+25 27 12.5	0.094	41.98	+47.22	1.35	
479.....	A2148 B	16 03 03.48	+25 27 09.3	0.094	41.96	+47.28	1.11	
480.....	A2148 C	16 03 52.47	+25 26 47.6	0.082	42.02	+47.10	1.17	
481.....	A2148 D	16 04 04.67	+25 33 45.3	0.082	42.20	+47.08	1.20	
482.....	A2148 E	16 02 30.36	+25 36 03.8	0.082	42.13	+47.43	1.08	
483.....	A2148 F	16 04 03.08	+25 29 48.5	0.082	42.10	+47.07	1.14	
484.....	A2148 1	16 03 22.26	+25 22 20.8	0.094	41.87	+47.19	0.97	
485.....	A2148 2	16 03 20.94	+25 18 32.2	0.094	41.78	+47.18	1.04	
486.....	A2148 3	16 02 47.85	+25 30 32.1	0.082	42.02	+47.35	1.04	
487.....	J18 A	16 04 56.79	+23 55 56.4	0.099	39.96	+46.49	1.80	NGC 6051
488.....	J18 B	16 05 17.71	+23 45 19.5	0.089	39.74	+46.37	1.33	
489.....	J18 C	16 04 50.62	+23 58 29.0	0.099	40.01	+46.53	1.27	
490.....	J18 D	16 03 41.91	+24 05 41.1	0.099	40.08	+46.81	1.15	
491.....	J18 E	16 04 46.89	+24 16 42.5	0.104	40.43	+46.62	1.15	
492.....	J18 F	16 05 49.60	+24 10 32.1	0.104	40.37	+46.36	1.15	
493.....	J18 1	16 06 23.28	+24 13 23.3	0.101	40.49	+46.25	1.15	
494.....	J18 2	16 05 06.54	+23 51 52.7	0.089	39.88	+46.44	1.15	
495.....	A2151 A	16 04 35.86	+17 43 15.9	0.025	31.47	+44.66	1.73	NGC 6041, VV 213a, 213b
496.....	A2151 B	16 04 39.62	+17 42 01.6	0.025	31.45	+44.64	1.52	NGC 6042
497.....	A2151 C	16 05 01.42	+17 46 31.9	0.037	31.60	+44.58	1.30	NGC 6043
498.....	A2151 D	16 05 09.04	+17 43 45.9	0.037	31.55	+44.54	1.49	NGC 6047
499.....	A2151 E	16 04 59.74	+17 52 12.0	0.037	31.72	+44.62	1.42	NGC 6044, IC 1172
500.....	A2151 F	16 05 44.72	+17 42 59.0	0.039	31.60	+44.40	1.42	IC 1185
501.....	A2151 G	16 06 32.23	+17 42 48.8	0.039	31.70	+44.22	1.42	IC 1193
502.....	A2151 H	16 06 39.39	+17 45 39.0	0.039	31.77	+44.21	1.42	IC 1194
503.....	A2151 I	16 05 46.38	+18 00 59.2	0.034	32.00	+44.50	1.42	
504.....	A2151 J	16 05 32.64	+18 09 33.0	0.032	32.16	+44.60	1.55	NGC 6055
505.....	A2151 K	16 05 39.71	+18 09 50.0	0.032	32.18	+44.58	1.30	NGC 6057
506.....	A2151 L	16 05 36.62	+18 16 21.2	0.032	32.32	+44.63	1.49	

TABLE 3—Continued

GIN	Name	R.A.	decl.	A_R	l (deg)	b (deg)	$\log D_w$	Comments
507.....	A2151 M	16 06 16.09	+18 14 58.7	0.049	32.36	+44.47	1.42	NGC 6061, IC 1190
508.....	A2151 N	16 06 06.15	+18 36 23.4	0.027	32.82	+44.63	1.25	
509.....	A2151 O	16 07 09.93	+18 38 27.4	0.034	32.98	+44.41	1.25	
510.....	A2151 1	16 07 38.61	+18 28 46.9	0.034	32.83	+44.25	1.19	
511.....	A2152 A	16 06 25.49	+15 41 07.2	0.037	29.07	+43.49	1.50	VV 215a
512.....	A2152 B	16 06 25.85	+15 41 36.5	0.037	29.08	+43.50	1.45	VV 215b
513.....	A2152 C	16 05 47.16	+15 47 26.2	0.037	29.12	+43.68	1.45	
514.....	A2152 D	16 04 51.79	+15 43 21.9	0.037	28.92	+43.85	1.55	
515.....	A2152 E	16 07 19.57	+15 50 57.9	0.037	29.39	+43.36	1.27	
516.....	A2152 F	16 05 15.15	+15 55 31.8	0.037	29.23	+43.85	1.32	
517.....	A2152 G	16 06 19.60	+16 25 52.0	0.051	30.01	+43.80	1.39	
518.....	A2152 H	16 05 29.24	+16 26 07.9	0.017	29.91	+43.99	1.42	
519.....	A2152 I	16 05 26.47	+16 26 35.3	0.017	29.92	+44.00	1.42	
520.....	A2152 J	16 04 41.19	+16 25 46.4	0.017	29.80	+44.16	1.27	
521.....	A2152 K	16 04 43.77	+16 31 19.4	0.017	29.93	+44.19	1.23	
522.....	A2152 L	16 04 49.94	+16 35 02.4	0.020	30.02	+44.19	1.35	
523.....	A2152 M	16 06 03.55	+16 10 31.4	0.041	29.65	+43.76	1.27	
524.....	A2152 N	16 06 16.55	+16 02 19.4	0.041	29.50	+43.66	1.23	
525.....	A2152 1	16 04 41.61	+16 38 56.9	0.020	30.09	+44.24	1.27	
526.....	A2152 2	16 06 58.41	+16 09 43.4	0.044	29.75	+43.55	1.23	
527.....	A2152 3	16 04 10.55	+16 05 13.9	0.025	29.30	+44.15	1.18	
528.....	P445-1 A	15 58 20.65	+18 04 49.7	0.037	31.20	+46.18	1.51	
529.....	P445-1 B	15 58 32.40	+17 52 16.2	0.037	30.94	+46.06	1.44	
530.....	P445-1 C	15 54 24.32	+18 39 05.8	0.034	31.51	+47.25	1.51	
531.....	P445-1 D	15 54 06.07	+18 38 51.0	0.032	31.46	+47.32	1.36	
532.....	P445-1 E	16 00 14.93	+18 22 32.6	0.034	31.83	+45.85	1.21	
533.....	P445-1 F	15 53 50.03	+18 20 27.6	0.032	31.01	+47.27	1.27	
534.....	P445-1 G	15 53 30.92	+18 21 27.6	0.032	30.99	+47.35	1.27	
535.....	P445-1 1	15 57 04.43	+17 37 31.7	0.053	30.43	+46.30	1.36	
536.....	P445-2 A	15 57 49.66	+16 18 35.0	0.051	28.77	+45.64	1.60	NGC 6023
537.....	P445-2 B	15 57 42.66	+16 13 04.0	0.051	28.63	+45.63	1.40	
538.....	P445-2 C	15 57 30.79	+15 57 20.8	0.032	28.26	+45.58	1.63	NGC 6021
539.....	P445-2 D	15 56 23.65	+16 31 22.6	0.032	28.86	+46.04	1.50	
540.....	A2162-N A	16 13 14.77	+30 54 08.8	0.032	50.38	+46.09	1.52	
541.....	A2162-N B	16 13 04.99	+30 54 05.0	0.032	50.37	+46.12	1.17	
542.....	A2162-N C	16 13 04.17	+30 54 00.4	0.032	50.37	+46.13	1.52	
543.....	A2162-N D	16 13 08.90	+30 49 37.0	0.032	50.27	+46.10	1.59	
544.....	A2162-N E	16 13 24.75	+30 35 58.0	0.032	49.96	+46.01	1.25	
545.....	A2162-N 1	16 12 57.06	+30 46 14.1	0.032	50.18	+46.13	1.32	
546.....	A2162-S A	16 12 35.61	+29 29 04.3	0.044	48.33	+46.01	1.73	NGC 6086
547.....	A2162-S B	16 11 58.88	+29 50 26.4	0.039	48.81	+46.20	1.60	
548.....	A2162-S C	16 11 55.34	+29 49 45.5	0.039	48.79	+46.21	1.41	
549.....	A2162-S D	16 12 16.76	+29 34 21.6	0.044	48.44	+46.09	1.15	
550.....	A2162-S E	16 12 11.31	+29 34 25.9	0.044	48.44	+46.11	1.57	
551.....	A2162-S F	16 11 56.69	+29 27 15.1	0.049	48.25	+46.14	1.30	
552.....	A2162-S G	16 12 38.94	+29 38 35.7	0.044	48.56	+46.02	1.49	
553.....	A2162-S H	16 11 29.61	+29 26 59.9	0.049	48.22	+46.24	1.23	
554.....	A2162-S I	16 11 02.05	+29 31 27.7	0.051	48.31	+46.35	1.30	
555.....	A2162-S 1	16 14 15.01	+29 17 31.5	0.053	48.15	+45.62	1.15	
556.....	A2162-S 2	16 11 36.32	+29 29 31.7	0.049	48.29	+46.22	1.15	
557.....	J20 A	16 18 00.61	+35 06 35.6	0.003	56.54	+45.57	1.32	NGC 6112
558.....	J20 B	16 17 40.60	+35 00 13.8	0.008	56.38	+45.63	1.49	NGC 6109
559.....	J20 C	16 17 20.19	+34 54 04.9	0.008	56.23	+45.69	1.66	NGC 6107
560.....	J20 D	16 17 09.39	+34 52 43.2	0.005	56.19	+45.72	1.52	NGC 6105
561.....	J20 E	16 18 23.70	+35 10 26.2	0.003	56.64	+45.49	1.46	NGC 6114
562.....	A2197 A	16 29 44.93	+40 48 39.7	0.000	64.68	+43.51	1.79	NGC 6173
563.....	A2197 B	16 27 41.20	+40 55 36.1	0.003	64.84	+43.90	1.55	NGC 6190
564.....	A2197 C	16 25 10.37	+40 53 33.1	0.003	64.79	+44.37	1.60	NGC 6146
565.....	A2197 D	16 30 41.91	+40 31 44.4	0.000	64.29	+43.32	1.25	Same as 576
566.....	A2197 E	16 30 33.98	+40 32 20.7	0.000	64.31	+43.35	1.42	NGC 6180
567.....	A2197 F	16 30 17.83	+40 35 53.0	0.000	64.39	+43.40	1.30	
568.....	A2197 G	16 29 23.84	+40 52 28.6	0.000	64.77	+43.57	1.25	A1627.7+40
569.....	A2197 H	16 28 54.21	+40 51 58.3	0.000	64.75	+43.67	1.19	
570.....	A2197 I	16 26 39.89	+40 28 39.7	0.008	64.21	+44.09	1.55	
571.....	A2197 J	16 28 37.98	+41 09 48.6	0.000	65.16	+43.72	1.19	
572.....	A2197 K	16 28 27.59	+41 09 38.3	0.000	65.16	+43.75	1.19	
573.....	A2197 L	16 28 41.72	+41 08 12.4	0.000	65.13	+43.71	1.19	
574.....	A2197 M	16 30 58.83	+40 55 48.4	0.000	64.85	+43.27	1.25	
575.....	A2197 N	16 28 21.60	+40 54 23.1	0.001	64.81	+43.77	1.25	
576.....	A2197 1	16 30 42.04	+40 31 45.1	0.000	64.30	+43.32	1.25	Same as 565
577.....	A2197 2	16 30 26.90	+41 29 01.9	0.003	65.61	+43.38	1.49	
578.....	A2197 3	16 29 09.44	+40 59 14.7	0.001	64.92	+43.62	1.25	
579.....	A2199 A	16 28 38.31	+39 33 03.3	0.000	62.93	+43.69	1.75	NGC 6166, VV 364

TABLE 3—Continued

GIN	Name	R.A.	decl.	A_R	l (deg)	b (deg)	$\log D_w$	Comments
580.....	A2199 B	16 28 23.40	+39 34 11.8	0.000	62.96	+43.74	1.27	NGC 6166C
581.....	A2199 C	16 27 58.76	+39 36 13.4	0.001	63.00	+43.82	1.27	
582.....	A2199 D	16 27 55.33	+39 15 30.1	0.000	62.52	+43.82	1.48	
583.....	A2199 E	16 33 49.71	+39 15 45.4	0.008	62.59	+42.68	1.42	IC 4610, IC 4612
584.....	A2199 F	16 31 02.84	+39 47 31.7	0.000	63.29	+43.24	1.53	
585.....	A2199 G	16 28 50.21	+39 50 04.7	0.003	63.33	+43.66	1.39	
586.....	A2199 H	16 31 19.30	+39 09 01.4	0.000	62.41	+43.16	1.27	
587.....	A2199 I	16 31 07.06	+39 12 17.8	0.000	62.48	+43.20	1.23	
588.....	A2199 J	16 30 45.32	+39 11 41.6	0.000	62.46	+43.27	1.27	
589.....	A2199 K	16 31 03.50	+39 50 17.6	0.000	63.35	+43.24	1.35	
590.....	A2199 L	16 27 40.96	+39 22 57.5	0.000	62.69	+43.87	1.48	NGC 6158
591.....	A2199 M	16 27 03.69	+39 31 37.5	0.003	62.89	+44.00	1.35	
592.....	A2199 N	16 27 22.16	+39 06 33.3	0.003	62.31	+43.92	1.53	
593.....	A2199 O	16 24 17.68	+39 12 39.4	0.000	62.43	+44.52	1.35	
594.....	A2199 P	16 23 28.15	+39 11 28.9	0.000	62.40	+44.68	1.35	
595.....	A2199 1	16 30 20.30	+39 48 15.0	0.001	63.30	+43.37	1.18	
596.....	A2199 2	16 29 56.67	+39 56 36.3	0.003	63.48	+43.45	1.23	
597.....	A2199 3	16 26 14.31	+39 58 00.9	0.001	63.50	+44.16	1.35	
598.....	J21 A	16 37 34.39	+50 20 42.0	0.000	77.52	+41.63	1.63	
599.....	J21 B	16 33 40.97	+50 22 28.8	0.000	77.66	+42.24	1.39	
600.....	J21 C	16 33 13.93	+50 23 53.9	0.000	77.71	+42.31	1.33	
601.....	J21 D	16 33 01.02	+50 23 41.5	0.000	77.71	+42.34	1.09	
602.....	J21 E	16 32 57.28	+50 24 05.3	0.000	77.72	+42.35	1.55	
603.....	J21 F	16 32 05.78	+50 22 45.5	0.000	77.71	+42.49	1.36	
604.....	J21 G	16 32 16.69	+50 11 21.0	0.000	77.45	+42.48	1.50	
605.....	J21 H	16 31 42.76	+50 14 10.4	0.000	77.53	+42.57	1.15	VV 687
606.....	J21 I	16 31 42.58	+50 10 03.1	0.000	77.44	+42.58	1.25	
607.....	J21 1	16 33 06.19	+50 32 08.6	0.000	77.89	+42.31	1.02	
608.....	J21 2	16 33 10.40	+50 18 21.5	0.000	77.58	+42.33	1.09	
609.....	A2247 A	16 52 48.57	+81 37 56.1	0.161	114.45	+31.01	1.35	
610.....	A2247 B	16 52 13.43	+81 37 10.6	0.161	114.44	+31.04	1.15	
611.....	A2247 C	16 51 45.53	+81 35 29.3	0.161	114.42	+31.06	1.23	
612.....	A2247 D	16 51 07.88	+81 34 56.1	0.161	114.43	+31.09	0.92	
613.....	A2247 E	16 50 59.18	+81 34 28.1	0.161	114.42	+31.10	1.15	
614.....	A2247 F	16 48 45.85	+81 36 37.8	0.161	114.50	+31.15	1.29	
615.....	A2247 1	17 01 42.70	+81 54 44.7	0.202	114.59	+30.61	1.05	
616.....	A2247 2	16 51 58.72	+81 30 42.2	0.161	114.34	+31.09	1.15	
617.....	P332-1 A	17 01 55.00	+28 25 01.9	0.169	49.95	+35.24	1.46	
618.....	P332-1 B	17 01 56.14	+28 23 15.5	0.169	49.92	+35.23	1.33	
619.....	P332-1 C	17 00 53.63	+27 43 27.4	0.142	49.06	+35.28	1.40	
620.....	P332-1 D	17 00 46.98	+27 50 55.4	0.152	49.20	+35.34	1.33	
621.....	P332-1 E	17 00 43.67	+28 01 31.8	0.152	49.41	+35.39	1.25	
622.....	P332-1 F	16 59 46.97	+27 46 01.1	0.157	49.04	+35.53	1.43	
623.....	P332-1 G	17 00 11.49	+28 16 45.1	0.152	49.67	+35.57	1.21	
624.....	P332-1 1	17 02 13.68	+28 07 43.9	0.157	49.63	+35.10	1.21	
625.....	P332-1 2	17 00 03.28	+28 25 40.4	0.147	49.84	+35.64	1.10	
626.....	J22 A	16 57 58.17	+27 51 14.1	0.157	49.01	+35.94	1.71	NGC 6269
627.....	J22 B	16 56 43.27	+27 49 17.9	0.166	48.89	+36.20	1.47	NGC 6263
628.....	J22 C	16 57 29.18	+27 50 38.3	0.157	48.97	+36.04	1.44	NGC 6265
629.....	J22 D	16 58 44.08	+27 51 31.6	0.157	49.07	+35.78	1.36	
630.....	J22 E	16 58 50.77	+27 57 52.7	0.157	49.21	+35.78	1.31	NGC 6271
631.....	J22 F	16 57 55.29	+27 41 56.7	0.140	48.82	+35.91	1.14	
632.....	J22 G	16 57 42.89	+27 39 32.1	0.140	48.76	+35.94	1.14	
633.....	J22 H	16 57 52.96	+28 07 41.2	0.157	49.33	+36.03	1.36	
634.....	J23 A	17 15 22.96	+57 24 39.8	0.044	85.81	+35.40	1.75	NGC 6338
635.....	J23 B	17 15 24.51	+57 19 20.8	0.037	85.70	+35.40	1.40	NGC 6346
636.....	J23 C	17 14 37.65	+57 18 19.4	0.017	85.69	+35.51	1.37	
637.....	J23 D	17 16 24.64	+57 25 16.9	0.044	85.81	+35.26	1.28	
638.....	J23 E	17 14 53.84	+57 40 21.6	0.049	86.13	+35.44	1.15	
639.....	J24 A	17 33 02.11	+43 45 33.0	0.041	69.52	+32.07	1.61	IC 1262
640.....	J24 B	17 33 08.86	+43 42 33.6	0.041	69.46	+32.05	1.25	
641.....	J24 C	17 33 21.53	+43 38 03.8	0.041	69.38	+32.00	1.18	IC 1264
642.....	J24 D	17 33 20.49	+43 54 46.9	0.046	69.71	+32.04	1.52	
643.....	J24 E	17 32 35.17	+43 51 08.8	0.046	69.61	+32.17	1.18	
644.....	J24 1	17 31 21.11	+43 36 57.1	0.041	69.30	+32.35	1.42	
645.....	J25 A	17 55 48.45	+62 36 42.2	0.106	91.82	+30.22	1.60	NGC 6521
646.....	J25 B	17 54 50.34	+62 38 40.1	0.106	91.85	+30.33	1.35	NGC 6512
647.....	J25 C	17 55 22.96	+62 39 28.2	0.106	91.87	+30.27	1.07	
648.....	J26 A	18 02 40.27	+42 47 42.7	0.082	69.60	+26.60	1.32	
649.....	J26 B	18 01 42.90	+42 43 07.8	0.070	69.47	+26.75	1.20	
650.....	J26 C	17 59 30.25	+42 30 54.0	0.056	69.14	+27.10	1.30	
651.....	J26 1	17 59 11.67	+42 35 27.8	0.056	69.21	+27.17	1.20	
652.....	J26 2	18 03 04.42	+42 57 21.2	0.082	69.79	+26.56	1.07	

TABLE 3—Continued

GIN	Name	R.A.	decl.	A_R	l (deg)	b (deg)	$\log D_w$	Comments
653.....	J27 A	18 36 20.76	+51 27 57.9	0.099	80.39	+23.15	1.71	
654.....	J27 B	18 35 58.69	+51 27 31.1	0.099	80.37	+23.21	1.57	
655.....	J27 C	18 34 05.01	+51 24 47.9	0.099	80.24	+23.48	1.39	
656.....	J27 D	18 36 51.50	+51 26 03.3	0.099	80.38	+23.07	1.37	
657.....	J27 E	18 36 52.29	+51 31 50.0	0.085	80.48	+23.09	1.17	
658.....	J38 A	21 41 03.96	−16 41 40.3	0.106	36.08	−44.90	1.41	
659.....	J38 B	21 40 57.65	−16 42 58.7	0.106	36.04	−44.89	1.23	
660.....	J38 C	21 42 15.95	−16 56 19.9	0.073	35.91	−45.26	1.36	
661.....	J38 1	21 42 01.58	−16 54 13.1	0.068	35.93	−45.19	1.27	
662.....	P522-1 A	22 50 02.23	+11 41 53.8	0.089	81.76	−41.27	1.76	NGC 7386
663.....	P522-1 B	22 49 54.69	+11 36 30.1	0.089	81.66	−41.32	1.68	NGC 7385
664.....	P522-1 C	22 49 25.31	+11 35 32.5	0.080	81.52	−41.26	1.20	
665.....	P522-1 D	22 49 35.70	+11 33 22.2	0.080	81.53	−41.32	1.50	NGC 7383
666.....	P522-1 E	22 49 46.00	+11 33 08.6	0.080	81.57	−41.35	1.11	
667.....	P522-1 F	22 50 19.62	+11 31 51.7	0.089	81.70	−41.45	1.28	NGC 7390
668.....	P522-1 G	22 50 17.73	+11 38 11.7	0.089	81.78	−41.36	1.46	NGC 7387
669.....	P522-1 1	22 51 28.23	+11 37 53.4	0.104	82.08	−41.53	1.20	
670.....	P522-1 2	22 51 09.04	+11 15 19.1	0.085	81.70	−41.79	1.11	
671.....	P522-1 3	22 49 21.56	+11 55 56.0	0.089	81.77	−40.98	1.28	
672.....	P522-1 4	22 49 10.26	+11 32 59.2	0.080	81.42	−41.26	1.35	
673.....	P522-1 5	22 48 55.55	+11 20 31.7	0.075	81.19	−41.39	0.98	
674.....	A2572 A	23 18 43.60	+18 41 52.7	0.080	94.28	−38.96	1.34	NGC 7602
675.....	A2572 B	23 18 33.27	+18 44 57.7	0.080	94.26	−38.90	1.23	NGC 7598
676.....	A2572 C	23 18 30.26	+18 41 19.5	0.080	94.22	−38.95	1.52	NGC 7597
677.....	A2572 D	23 19 13.34	+18 54 40.4	0.070	94.54	−38.82	1.21	
678.....	A2572 E	23 17 21.45	+18 56 28.4	0.092	94.05	−38.60	1.12	
679.....	A2572 1	23 18 39.28	+18 41 21.3	0.080	94.26	−38.96	1.06	
680.....	A2572 2	23 18 29.45	+18 37 15.8	0.092	94.17	−39.00	0.93	
681.....	A2589 A	23 23 57.48	+16 46 36.7	0.029	94.62	−41.24	1.73	NGC 7647
682.....	A2589 B	23 23 59.18	+16 48 39.4	0.029	94.65	−41.21	1.29	
683.....	A2589 C	23 23 48.23	+16 46 07.0	0.029	94.57	−41.23	1.21	
684.....	A2589 D	23 23 54.47	+16 40 50.2	0.029	94.55	−41.32	1.16	
685.....	A2589 E	23 23 51.43	+16 38 41.6	0.029	94.51	−41.34	1.35	
686.....	A2589 F	23 23 50.89	+16 53 48.3	0.029	94.66	−41.12	1.21	
687.....	A2589 G	23 23 47.68	+16 51 07.9	0.029	94.62	−41.15	1.05	
688.....	A2589 H	23 23 58.99	+16 52 29.1	0.029	94.68	−41.15	0.90	
689.....	A2589 1	23 24 19.65	+16 43 53.7	0.029	94.70	−41.32	1.05	
690.....	A2589 2	23 23 10.61	+16 54 45.5	0.041	94.48	−41.03	1.05	
691.....	A2593-N A	23 24 20.20	+14 38 48.8	0.065	93.45	−43.18	1.68	NGC 7649
692.....	A2593-N B	23 24 12.24	+14 37 06.7	0.065	93.39	−43.19	1.22	
693.....	A2593-N C	23 24 32.21	+14 38 20.2	0.065	93.50	−43.21	1.16	
694.....	A2593-N D	23 24 37.33	+14 38 31.8	0.065	93.53	−43.22	1.22	
695.....	A2593-N E	23 24 41.30	+14 37 58.1	0.065	93.54	−43.23	1.46	IC 1487
696.....	A2593-N F	23 24 23.10	+14 39 29.9	0.065	93.47	−43.18	1.08	
697.....	A2593-N G	23 24 39.82	+14 40 01.2	0.065	93.55	−43.20	1.19	
698.....	A2593-N H	23 24 35.89	+14 40 57.0	0.065	93.55	−43.18	1.19	
699.....	A2593-N I	23 24 23.70	+14 42 23.9	0.065	93.50	−43.14	1.22	
700.....	A2593-N J	23 24 12.15	+14 25 25.2	0.061	93.27	−43.37	1.31	
701.....	A2593-N K	23 24 42.84	+14 31 05.0	0.063	93.48	−43.34	1.36	
702.....	A2593-N L	23 25 37.66	+14 34 24.8	0.063	93.78	−43.39	1.16	
703.....	A2593-N M	23 25 24.85	+14 45 23.1	0.068	93.83	−43.20	1.22	
704.....	A2593-N 1	23 24 36.87	+14 35 00.5	0.065	93.49	−43.27	1.16	
705.....	A2593-N 2	23 24 28.45	+14 41 40.5	0.065	93.52	−43.16	0.92	
706.....	A2593-N 3	23 24 01.52	+14 28 52.7	0.061	93.25	−43.30	1.03	
707.....	A2593-N 4	23 23 33.56	+14 34 35.3	0.065	93.17	−43.16	1.03	
708.....	A2593-N 5	23 23 11.85	+14 54 03.7	0.065	93.27	−42.83	1.22	
709.....	A2593-S A	23 24 26.11	+13 58 18.1	0.061	93.05	−43.79	1.61	NGC 7651
710.....	A2593-S B	23 24 49.11	+13 59 46.1	0.061	93.18	−43.82	1.28	
711.....	A2593-S C	23 24 16.69	+13 57 58.8	0.061	93.00	−43.78	1.31	
712.....	A2593-S D	23 24 31.86	+14 16 18.3	0.061	93.27	−43.54	1.26	
713.....	A2593-S E	23 23 26.77	+14 07 52.6	0.061	92.86	−43.54	1.35	
714.....	A2593-S F	23 24 03.51	+13 56 51.1	0.061	92.92	−43.77	1.06	
715.....	A2593-S G	23 23 55.54	+13 54 36.6	0.061	92.86	−43.79	1.13	
716.....	A2634 A	23 38 29.53	+27 01 53.0	0.097	103.50	−33.07	1.84	NGC 7720
717.....	A2634 B	23 38 38.90	+27 00 39.5	0.087	103.53	−33.10	1.34	IC 5342
718.....	A2634 C	23 38 29.34	+26 58 42.1	0.087	103.48	−33.12	1.31	
719.....	A2634 D	23 38 26.90	+26 59 04.6	0.087	103.47	−33.11	1.31	IC 5341
720.....	A2634 E	23 38 50.79	+27 16 01.0	0.097	103.68	−32.88	1.47	
721.....	A2634 F	23 37 57.93	+27 15 50.9	0.109	103.46	−32.81	1.31	
722.....	A2634 G	23 40 00.95	+27 07 58.6	0.104	103.92	−33.09	1.68	NGC 7728
723.....	A2634 H	23 40 46.92	+26 50 04.3	0.082	104.00	−33.43	1.55	A2338 + 26
724.....	A2634 I	23 39 49.50	+27 22 31.9	0.104	103.97	−32.85	1.31	
725.....	A2634 J	23 40 19.15	+27 33 39.5	0.111	104.17	−32.71	1.59	

TABLE 3—Continued

GIN	Name	R.A.	decl.	A_R	l (deg)	b (deg)	$\log D_W$	Comments
726.....	A2634 K	23 40 54.43	+27 30 32.5	0.111	104.29	−32.80	1.34	
727.....	A2634 1	23 38 22.88	+27 09 27.8	0.097	103.52	−32.95	1.31	
728.....	A2634 2	23 38 18.63	+26 53 11.2	0.087	103.40	−33.20	1.34	
729.....	A2657 A	23 44 57.45	+09 11 33.9	0.133	96.72	−50.26	1.57	
730.....	A2657 B	23 44 43.91	+09 12 55.2	0.133	96.65	−50.22	1.13	
731.....	A2657 C	23 44 30.50	+09 15 48.2	0.133	96.60	−50.16	1.32	
732.....	A2657 D	23 44 27.78	+09 16 00.2	0.133	96.59	−50.15	0.91	
733.....	A2657 E	23 44 24.69	+09 09 51.9	0.133	96.51	−50.24	1.23	
734.....	A2657 F	23 44 16.22	+09 02 54.2	0.133	96.39	−50.33	1.33	
735.....	A2657 G	23 45 01.73	+09 02 39.8	0.133	96.65	−50.41	0.99	
736.....	A2657 H	23 45 17.34	+09 16 16.4	0.133	96.89	−50.23	1.18	
737.....	A2657 1	23 45 40.65	+09 14 06.3	0.133	97.00	−50.30	1.18	
738.....	A2666 A	23 50 58.70	+27 08 48.5	0.080	106.72	−33.81	1.79	NGC 7768
739.....	A2666 B	23 50 52.42	+27 09 56.9	0.080	106.69	−33.79	1.36	NGC 7765
740.....	A2666 C	23 51 01.30	+27 15 26.1	0.080	106.76	−33.71	1.20	
741.....	A2666 D	23 51 00.92	+27 17 18.8	0.061	106.77	−33.68	1.28	
742.....	A2666 E	23 51 30.16	+27 14 08.5	0.065	106.88	−33.76	1.36	
750.....	COMA 70	12 59 07.91	+27 46 10.7	0.024	53.97	+88.18	1.34	IC 3957
751.....	COMA 69	12 59 07.90	+27 47 01.7	0.024	54.38	+88.17	1.46	IC 3959
752.....	COMA 240	12 57 31.89	+28 28 16.0	0.026	78.18	+88.10	1.63	NGC 4841A
753.....	COMA 239	12 57 33.88	+28 28 54.0	0.026	78.26	+88.08	1.46	NGC 4841B
754.....	COMA 194	12 59 03.79	+28 07 25.6	0.031	63.89	+88.04	1.62	NGC 4860
755.....	COMA 159	12 59 12.82	+27 58 37.8	0.031	59.60	+88.08	1.52	NGC 4864
756.....	COMA 133	12 59 14.82	+27 58 13.8	0.031	59.33	+88.08	1.44	NGC 4867
757.....	COMA 105	12 59 22.82	+27 54 44.0	0.031	57.39	+88.07	1.52	NGC 4869
758.....	COMA 31	12 57 24.27	+27 29 47.9	0.014	48.81	+88.62	1.67	NGC 4839
759.....	COMA 49	13 01 54.45	+27 37 28.8	0.024	45.59	+87.62	1.55	NGC 4926
760.....	COMA 87	12 59 30.84	+27 47 35.1	0.024	53.76	+88.09	1.19	
761.....	COMA 103	12 59 30.81	+27 53 03.1	0.024	56.28	+88.06	1.42	IC 3973
762.....	COMA 106	12 59 22.82	+27 53 49.0	0.031	56.97	+88.08	1.30	
763.....	COMA 107	12 59 20.83	+27 53 15.0	0.031	56.79	+88.09	1.40	
764.....	COMA 118	13 00 39.62	+27 55 21.4	0.029	54.69	+87.81	1.49	NGC 4906
765.....	COMA 129	12 59 34.77	+27 57 38.2	0.029	58.16	+88.01	1.96	NGC 4874
766.....	COMA 134	12 59 03.85	+27 57 32.6	0.031	59.54	+88.12	1.19	
767.....	COMA 135	12 58 59.86	+27 58 02.6	0.031	59.97	+88.13	1.12	
768.....	COMA 136	12 58 55.87	+27 58 01.5	0.031	60.16	+88.14	1.16	
769.....	COMA 148	13 00 07.68	+27 58 32.8	0.029	57.18	+87.90	2.08	NGC 4889
770.....	COMA 160	12 59 05.83	+27 59 47.7	0.031	60.46	+88.09	1.57	IC 3955
771.....	COMA 172	13 00 13.64	+28 02 20.9	0.029	58.50	+87.85	1.36	IC 4021
772.....	COMA 217	12 59 57.60	+28 14 50.6	0.034	64.10	+87.81	1.60	NGC 4881
773.....	N3379	10 47 49.50	+12 34 56.9	0.029	233.49	+57.63	...	
774.....	N936	02 27 37.67	−01 09 17.2	0.029	168.57	−55.26	...	
775.....	N3115	10 05 13.42	−07 43 06.5	0.058	247.78	+36.78	...	
776.....	N3377	10 47 42.05	+13 59 09.1	0.036	231.18	+58.32	...	
777.....	N4365	12 24 27.87	+07 19 04.9	0.000	283.80	+69.18	...	
778.....	N4374	12 25 03.15	+12 53 11.2	0.074	278.20	+74.48	...	
779.....	N4382	12 25 24.23	+18 11 23.4	0.017	267.72	+79.24	...	
780.....	N4406	12 26 11.07	+12 56 47.7	0.067	279.07	+74.64	...	
781.....	N4472	12 29 46.57	+08 00 07.5	0.000	286.92	+70.20	...	
782.....	N4473	12 29 47.75	+13 25 49.6	0.036	281.60	+75.40	...	
783.....	N4486B	12 30 31.85	+12 29 26.0	0.053	283.41	+74.56	...	
784.....	N4494	12 31 23.50	+25 46 32.5	0.031	228.58	+85.31	...	
785.....	COMA 130	12 59 33.78	+27 56 50.2	0.029	57.85	+88.02	1.49	NGC 4872
786.....	COMA 153	12 59 43.73	+27 59 47.4	0.029	58.70	+87.97	1.30	
787.....	COMA 124	12 59 43.77	+27 54 44.4	0.029	56.51	+88.00	1.49	NGC 4876
788.....	COMA 125	12 59 42.76	+27 55 37.4	0.029	56.94	+88.00	1.27	
789.....	COMA 143	13 00 52.56	+28 00 21.7	0.029	56.24	+87.73	1.60	IC 4051
790.....	COMA 168	13 00 48.54	+28 05 21.6	0.034	58.31	+87.71	1.51	IC 4045
791.....	COMA 151	13 00 03.69	+27 59 08.7	0.029	57.59	+87.91	1.56	NGC 4886
792.....	COMA 150	13 00 06.67	+28 00 08.8	0.029	57.89	+87.89	1.36	IC 4011
793.....	COMA 174	13 00 07.64	+28 04 38.8	0.029	59.68	+87.85	1.39	IC 4012
794.....	N584	01 31 21.01	−06 52 16.1	0.065	149.81	−67.64	...	
795.....	N596	01 32 52.08	−07 01 54.6	0.062	150.89	−67.63	...	
796.....	N4697	12 48 35.71	−05 48 02.9	0.022	301.63	+57.06	...	
797.....	N5846	15 06 28.73	+01 36 15.6	0.084	0.42	+48.80	...	
798.....	N6181	16 32 21.00	+19 49 35.6	0.137	37.17	+39.21	...	
799.....	N7626	23 20 42.29	+08 13 02.5	0.096	87.86	−48.38	...	
800.....	N4486	12 30 49.24	+12 23 32.1	0.053	283.77	+74.49	...	
801.....	N224	00 42 44.23	+41 16 07.7	0.187	121.17	−21.57	...	

NOTE.—Units of right ascension are hours, minutes, and seconds, and units of declination are degrees, arcminutes, and arcseconds (J2000).

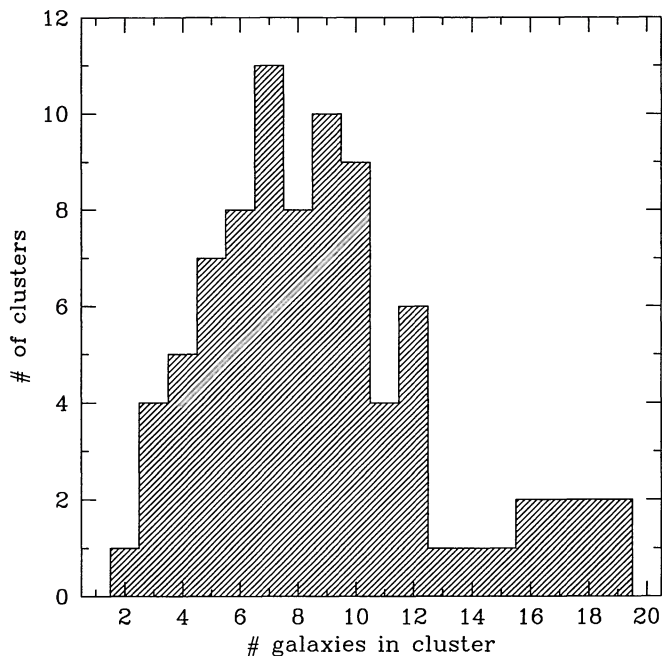


FIG. 4.—Distribution of the number of galaxies selected in each program cluster.

tions obtained appear to have an accuracy of 0.5 and were checked repeatedly during acquisition at the telescope. The R -band extinctions given in Table 3 were computed according to $A_R = 2.4E(B-V)$, with $E(B-V)$ obtained from Burstein & Heiles (1982, 1984).

4. SAMPLE SELECTION FUNCTIONS

It has long been known, starting with Malmquist (1920), Neyman & Scott (1959), and others, that the statistical properties of a sample of objects depends on a number of observational factors, including the cutoff and completeness of the sample. In investigations of this kind, there are two levels of selection we must deal with: (1) the choice of the clusters (or “fields”), and (2) the selection of the galaxies themselves. Having dealt with the former in § 2, we now turn to quantifying the latter.

Incompleteness among the small, faint galaxies observed in a given cluster can lead to a strong selection bias, which affects the estimated distance to the cluster (see Lynden-Bell et al. 1988; Willick 1994; Strauss & Willick 1995; Freudling et al. 1995). As each cluster has its own intrinsic distance, richness, and structure, it will also have its own selection function that depends on the observational quantity upon which the sample is selected. The relevant quantity in this study is the photographic diameter measured from the Sky Survey images.

For a cluster of galaxies, with index j , found within a fixed solid angle on the sky, we estimated the selection function of the survey (the completeness as a function of the selection variable X), $S_j(X)$, by binning the program elliptical galaxies in k fixed intervals ΔX and summing the number in each bin. We excluded program galaxies found to be spirals or otherwise unusable in our subsequent CCD imaging, as these will not be used for obtaining distances and so should not be included in the selection function. This yields the count, $N_{j,k}^{\text{obs}}$, of observed galaxies with the range of desired morphological types belonging to cluster j in the interval

$X_k - \frac{1}{2}\Delta X \leq X_k < X_k + \frac{1}{2}\Delta X$. The ratio of this value to the true number of galaxies in this cluster and interval with the range of desired morphological types, $N_{j,k}^{\text{all}}$, yields the selection function,

$$S_j(X_k) = N_{j,k}^{\text{obs}}(X_k)/N_{j,k}^{\text{all}}(X_k). \quad (1)$$

In order to estimate $N_{j,k}^{\text{all}}$ and thus determine S_j , a second catalog of all galaxies that *might* have been in the sample must be constructed. This means, for each cluster, measuring the photographic diameters for all elliptical galaxies (spirals were excluded) as large as or larger than the smallest galaxy that is included in our sample.

The method for selecting candidate galaxies simply consisted of choosing, by eye, objects larger than some size that looked like elliptical galaxies on our high-quality photographic enlargements of the glass copies of the Sky Survey plates. This selection procedure can be quantified by measuring optical major-axis diameters D_W (in arcseconds) for every elliptical-like galaxy in all the cluster fields (including both the galaxies in the sample and other, mostly smaller, galaxies in the same fields). These diameters were measured in a homogeneous fashion by G. W. off the photographic enlargements of the Sky Survey glass copies. In all, 2185 diameter measurements were made; those for the program galaxies are listed in Table 3. These D_W 's are a good measure of the true sizes of the galaxies, as illustrated by Figure 5, which, using preliminary estimates of D_R (the diameter enclosing a mean surface brightness of 20.5 mag arcsec⁻² in the Kron-Cousins R band), shows the good correlation that exists between $\log D_W$ and $\log D_R$. The full details of the derivation of the D_R -values will be given in Paper III, on the photometry (Saglia et al. 1996).

The selection function for each cluster j was computed from the ratio of the $\log D_W$ distributions (with $\Delta \log D_W = 0.2$ dex binning) of the EFAR program galaxies

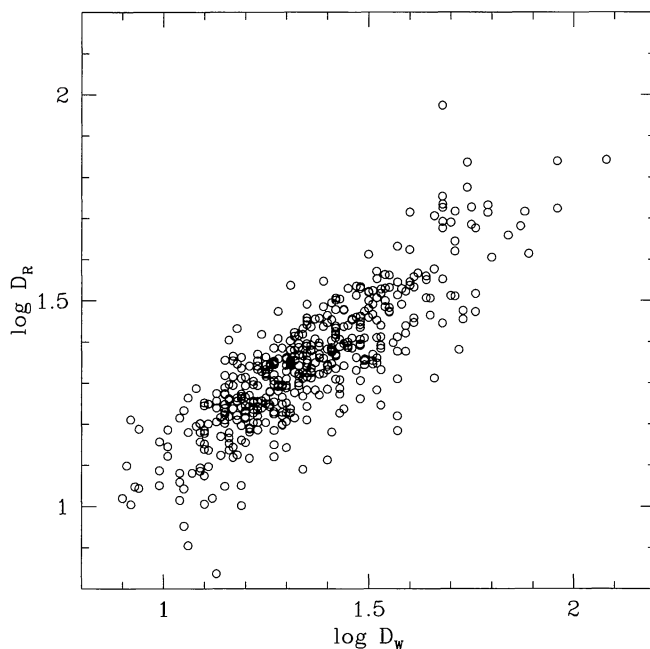


FIG. 5.—Relation between $\log D_W$ (diameters measured by hand) and $\log D_R$ (photometric diameter at fixed surface brightness) for the entire galaxy sample, without allowing for offsets between clusters due to differences in extinction, plate-to-plate zero points, etc.

(with spirals omitted), N_j^{EFAR} , and *all* galaxies with measured D_W , N_j^{all} :

$$S_j(\log D_W) = N_j^{\text{EFAR}}(\log D_W) / N_j^{\text{all}}(\log D_W). \quad (2)$$

To characterize the selection function $S_j(\log D_W)$, we follow Neyman & Scott (1959) and Willick (1994) and adopt the useful form

$$S_j(\log D_W) = 0.5 \{ 1 + \text{erf} [(\log D_W - \log D_{W,j}^0) / \delta_{W,j}] \}, \quad (3)$$

where $\log D_{W,j}^0$ is the midpoint, and $\delta_{W,j}$ the width, of the cutoff in the selection function. In practice, we fitted this

relation by performing a linear least-squares fit to

$$\text{erf}^{-1} [2S_j(\log D_W) - 1] = (\log D_W - \log D_{W,j}^0) / \delta_{W,j}, \quad (4)$$

where erf^{-1} denotes the inverse error function. For some of the clusters, there were too few points to fit both parameters, so we used the mean width $\langle \delta_W \rangle = 0.24$ and determined only the cutoff $\log D_W^0$. The uncertainty in $\log D_W^0$ is dominated by the small numbers of galaxies in each cluster and is ~ 0.1 dex. Example selection functions for some of the clusters are shown in Figure 6. Note that the cutoff in the selection function for Coma is particularly broad, as a

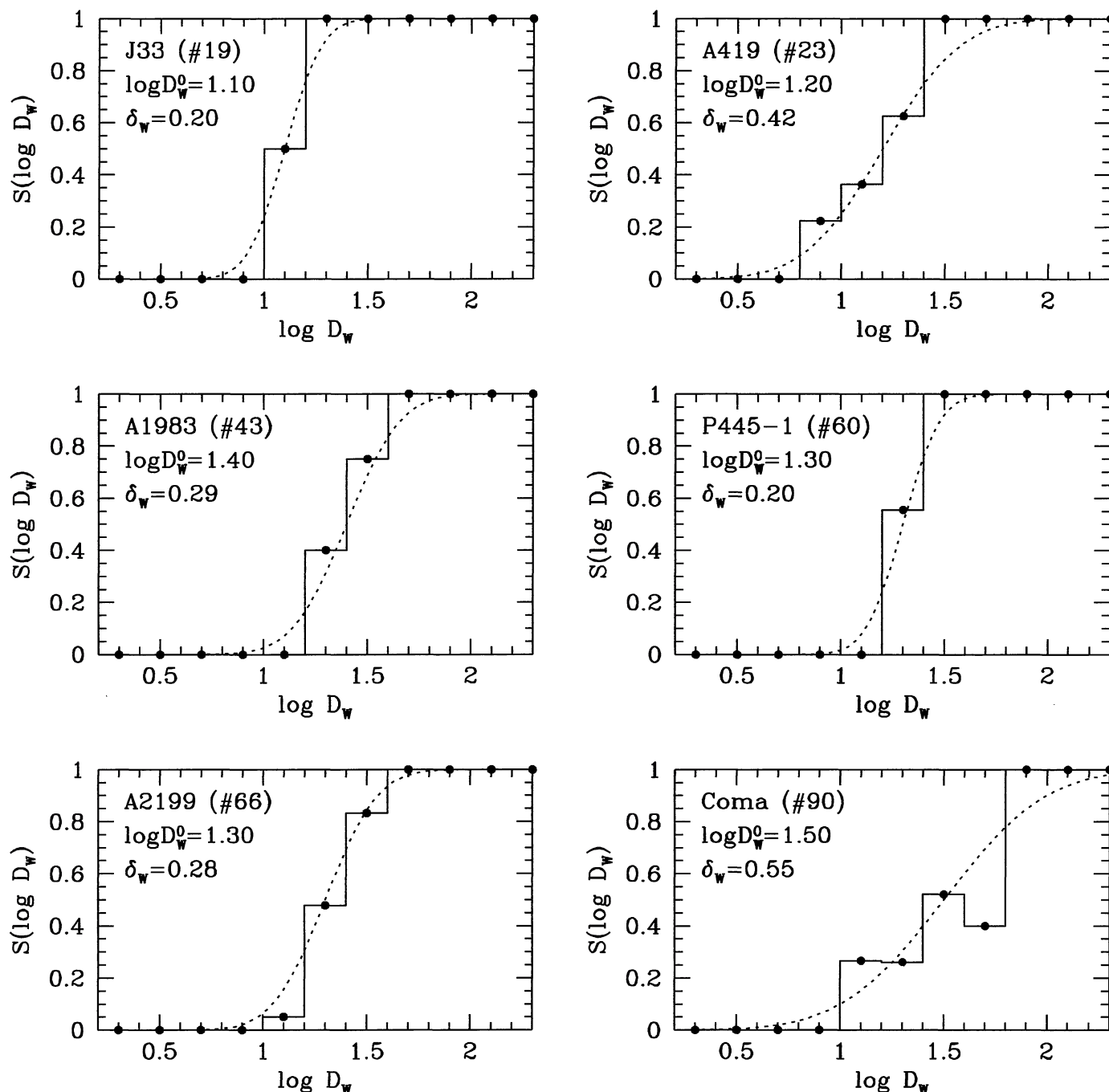


FIG. 6.—Examples of the selection functions for some individual galaxy clusters. The dots and histograms show the selection function for elliptical galaxies measured for the cluster whose name is in the upper left corner of each panel. The dashed curves give the fit to these data using eq. (3) with the cutoff and slope parameters D_W^0 and δ_W .

result of the fact that the galaxies in Coma were not selected in the same way as the other clusters but were simply garnered from the literature of previous observations in the cluster.

Our estimates of the selection functions for each cluster are valid as long as (1) the diameters measured for all galaxies are as small as or smaller than the smallest program galaxy in the cluster and (2) the two samples are not badly contaminated by galaxies of the wrong morphological types. Figure 7a shows that this first requirement is satisfied, for the catalog of all $\log D_w$ diameters (*hatched histogram*) only begins to show incompleteness at ~ 0.2 dex below the cutoff $\log D_w^0$ in the sample of program galaxies in each cluster.

The second potential source of error in the galaxy counts, stemming from the difficulty of assigning correct types to the smallest galaxies, could produce a systematic change in the contamination by spirals with diameter. However, this will be approximately compensated if the fractions of incorrectly selected galaxies are similar in the two catalogs. This is shown to be the case in Figure 7b, which compares the distributions of rejected spirals from the two samples. Here the two distributions have nearly the same shape, and their ratio remains nearly constant at ~ 0.5 near the cutoff of the selection functions. The final morphological types will be given in the photometry paper (Saglia et al. 1996). Here we are concerned purely with the initial sample selection; this involved the by-eye morphologies but not the detailed CCD image-based classifications, which will be discussed in later papers.

The combined selection function for the entire sample, correcting for differences in $\log D_w$ between clusters, is shown in Figure 8. The selection function corresponding to the mean parameters $\langle \log D_w^0 \rangle = 1.25$ and $\langle \delta_w \rangle = 0.24$ (i.e., cluster-weighted by using the subsample of clusters for

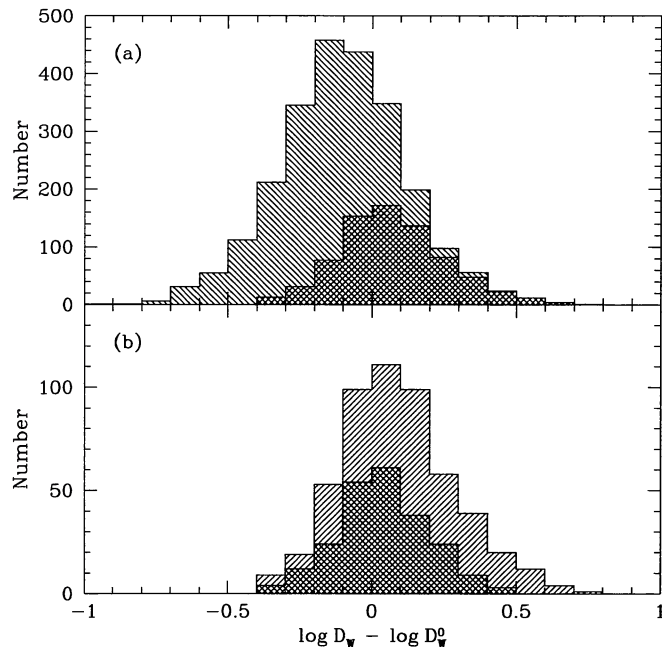


FIG. 7.—(a) Distributions of $\log D_w - \log D_w^0$ for the complete set of objects (E, S0, and cD galaxies) with D_w diameter measurements from the POSS prints (*hatched histogram*) and for the subset of the EFAR program galaxies only (*cross-hatched histogram*). (b) The corresponding distributions of spirals rejected from the two samples.

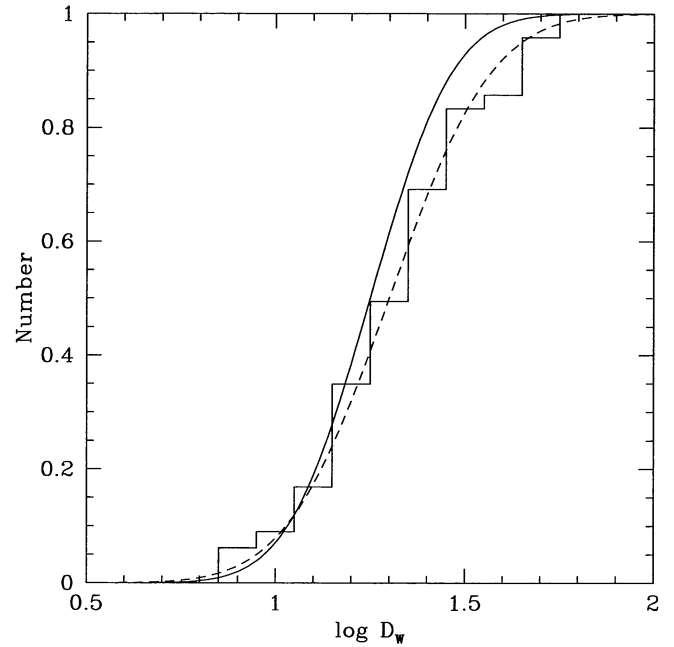


FIG. 8.—Combined selection function for the entire sample, with each cluster's selection function shifted to the mean $\log D_w^0$. The solid curve has $\langle \log D_w^0 \rangle = 1.2$ and $\langle \delta_w \rangle = 0.24$, the mean parameters averaged over all the clusters. The dashed curve has $\log D_w^0 = 1.30$ and $\delta_w = 0.30$ and is the fit to the combined selection function.

which we could directly determine these parameters) is shown by the solid curve. Fitting the combined galaxy sample directly yields the dashed curve, which is the galaxy-weighted selection function; it has a slightly higher cutoff, $\log D_w^0 = 1.30$, and is slightly broader, $\delta_w = 0.30$. Thus the selection functions typically have a cutoff at $\langle D_w^0 \rangle = 18''$ – $20''$ and drop from 90% to 10% completeness over a range of $1.8\langle \delta_w \rangle = 0.44$ – 0.54 dex (i.e., between $30''$ and $10''$). Figure 9 shows that the selection is indeed by angular diameter: note the curves of constant angular size produced by the discreteness of the $\log D_w^0$ estimates. Over the range from 6000 to $15,000 \text{ km s}^{-1}$, a typical cutoff diameter of $19''$ corresponds to a metric diameter increasing from 11 to 28 kpc (for $H_0 = 50 \text{ km s}^{-1} \text{ Mpc}^{-1}$).

The selection regions and the parameters of the selection functions for all clusters are listed in Table 4. The CIDs in the first column correspond to those in Table 1. The solid angles on the sky that were surveyed for each cluster were measured from the photographic prints, and with the exception of two clusters, the fields are rectangles running east-west and north-south. Thus, we measured the right ascension and declination of the center of each rectangle (not the same as the cluster centers in Table 1) and the total length and height, $\Delta\alpha$ and $\Delta\delta$, of the sides of these rectangles (in units of arcminutes), which are given in the second through fifth columns, respectively. The selection function parameters N_w (the total number of D_w diameters measured in each field), $\log D_w$, and δ_w are listed in the final three columns.

In subsequent papers, we will apply additional selection criteria (such as the availability of spectroscopic and photometric observations or morphological criteria based on the CCD imaging) in order to refine the initial program sample. We will then compute the corresponding new selection functions, using the method described above. In general we

TABLE 4
SELECTION REGIONS AND SELECTION FUNCTION PARAMETERS

CID	R.A.	decl.	$\Delta\alpha$ (arcmin)	$\Delta\delta$ (arcmin)	N_W	$\log D_W^0$	δ_W
1.....	00 39.4	+06 54	83.22	92.15	28	1.3	0.20
2.....	00 42.1	−09 32	67.41	53.12	26	1.3	0.24
3.....	00 56.4	−01 05	58.66	81.38	49	1.4	0.24
4.....	00 59.9	+27 00	99.38	51.42	29	1.2	0.23
5.....	00 58.9	+12 56	48.16	38.85	20	1.2	0.20
6.....	01 08.6	+02 11	62.01	44.76	23	1.1	0.20
7.....	01 12.3	+15 32	81.74	47.44	48	1.4	0.24 ^a
7.....	01 12.2	+16 20	68.86	45.10	^a
8.....	01 14.8	+00 08	79.65	65.17	27	1.2	0.22
9.....	01 24.8	+01 47	65.19	44.52	21	1.4	0.20
10.....	01 20.6	−13 47	41.92	30.58	34	1.2	0.36
11.....	01 25.0	+08 44	50.42	47.47	25	1.1	0.20
12.....	01 37.5	−09 06	58.91	50.16	19	1.2	0.26
13.....	01 50.7	+33 15	64.38	50.55	16	1.2	0.21
14.....	01 53.9	+36 11	126.25	113.05	31	1.6	0.21
15.....	02 25.1	+37 06	41.03	38.28	9	1.1	0.20
16.....	02 29.7	+23 04	65.53	34.73	23	1.2	0.24
17.....	02 45.9	+36 59	56.48	51.29	24	1.1	0.20
18.....	02 50.6	+47 00	64.13	41.96	20	1.3	0.27
19.....	02 55.5	−14 12	58.14	45.45	8	1.1	0.20
20.....	02 57.3	+16 03	56.26	39.74	22	1.3	0.24
21.....	02 58.0	+06 10	88.06	58.27	25	1.3	0.20
22.....	03 08.5	−04 09	64.73	51.10	12	1.2	0.20
23.....	03 08.4	−23 35	36.55	39.63	33	1.2	0.42
24.....	04 33.9	−13 13	75.26	54.96	27	1.4	0.24
25.....	04 45.6	−15 57	75.49	70.34	32	1.4	0.24
26.....	04 52.8	+01 18	32.99	27.32	5	1.3	0.20
27.....	04 58.8	−00 23	45.41	41.32	12	1.1	0.20
28.....	04 55.0	−18 04	79.41	69.31	23	1.3	0.20
29.....	04 49.8	−17 05	89.69	68.17	20	1.3	0.20
30.....	04 60.4	−18 32	48.42	51.33	20	1.2	0.21
31.....	05 03.5	−20 11	44.98	42.57	8	1.1	0.20
32.....	05 04.8	−19 15	50.04	41.59	15	1.1	0.20
33.....	05 03.2	−23 57	98.88	72.28	44	1.3	0.24
34.....	05 01.6	−22 56	72.36	76.31	25	1.4	0.36
35.....	05 47.9	−25 27	80.87	58.78	39	1.3	0.22 ^b
36.....	05 43.5	−25 55	75.53	53.15	60	1.3	0.20 ^c
37.....	13 05.7	+53 43	58.00	45.96	21	1.3	0.27
38.....	13 43.3	+29 58	67.89	51.79	21	1.2	0.24
39.....	13 53.3	+25 00	93.08	49.85	32	1.2	0.21
40.....	14 08.3	−09 02	57.22	40.96	23	1.2	0.24
41.....	14 47.3	+13 40	57.67	41.53	23	1.1	0.24
42.....	14 47.7	+11 23	66.61	52.49	30	1.3	0.20
43.....	14 51.8	+16 45	76.32	55.66	30	1.4	0.29
44.....	14 53.2	+18 28	85.88	54.83	43	1.3	0.22
45.....	15 19.2	+04 27	83.60	50.03	16	1.1	0.20
46.....	15 10.9	+04 29	118.93	50.22	50	1.3	0.24
47.....	15 21.9	+08 08	47.57	60.07	10	1.5	0.24
48.....	15 11.7	+07 35	80.74	67.48	27	1.2	0.24
49.....	15 17.1	+07 02	64.95	47.19	33	1.4	0.24
50.....	15 23.7	+08 57	92.42	75.62	22	1.3	0.24
51.....	15 39.1	+21 44	56.20	48.24	24	0.9	0.24
52.....	15 54.6	+41 34	42.35	32.71	25	1.1	0.20
53.....	16 01.9	+16 07	59.01	84.49	32	1.5	0.24
54.....	15 57.3	+22 30	36.49	31.14	8	1.1	0.20
55.....	16 11.6	+23 59	41.84	37.66	12	1.2	0.24
56.....	16 03.3	+25 28	31.27	30.00	23	1.0	0.22
57.....	16 05.1	+23 58	40.78	38.97	31	1.3	0.24
58.....	16 05.9	+18 09	69.42	68.28	49	1.4	0.24
59.....	16 06.1	+16 08	58.37	83.84	65	1.3	0.34
60.....	15 57.0	+18 08	105.42	71.07	38	1.3	0.20
61.....	15 57.9	+16 07	52.24	84.17	16	1.4	0.20
62.....	16 13.1	+30 58	57.71	49.03	27	1.1	0.20
63.....	16 12.8	+29 32	60.51	46.34	42	1.2	0.24
64.....	16 17.6	+35 01	78.37	69.19	26	1.5	0.23
65.....	16 28.2	+40 55	117.87	72.36	27	1.3	0.42
66.....	16 28.5	+39 29	125.14	61.31	54	1.3	0.28
67.....	16 34.0	+50 25	76.86	57.42	12	1.3	0.24
68.....	16 50.8	+81 43	57.62	45.47	12	1.0	0.24
69.....	17 01.2	+28 03	46.12	59.88	20	1.2	0.24
70.....	16 57.6	+27 54	45.15	38.53	15	1.3	0.24
71.....	17 15.4	+57 28	50.62	52.49	16	1.2	0.22

TABLE 4—Continued

CID	R.A.	decl.	$\Delta\alpha$ (arcmin)	$\Delta\delta$ (arcmin)	N_W	$\log D_W^0$	δ_W
72.....	17 33.1	+43 50	42.18	41.96	19	1.3	0.24
73.....	17 55.5	+62 41	41.03	38.28	17	1.2	0.24
74.....	18 01.5	+42 44	70.69	42.88	14	1.3	0.24
75.....	18 36.4	+51 35	49.78	40.37	11	1.2	0.30
76.....	21 41.2	−16 43	64.49	46.69	14	1.2	0.20
77.....	22 50.1	+11 41	43.67	54.04	16	1.1	0.20
78.....	23 18.1	+18 48	35.84	31.62	24	1.3	0.24
79.....	23 23.9	+16 49	31.17	26.64	23	1.1	0.20
80.....	23 24.8	+14 42	45.98	38.09	34	1.1	0.24
81.....	23 24.7	+14 04	43.14	31.79	18	1.2	0.24
82.....	23 39.2	+27 10	60.11	50.49	30	1.3	0.20
83.....	23 45.0	+09 14	33.11	29.12	16	1.1	0.24
84.....	23 51.4	+27 14	39.43	29.23	18	1.2	0.24
90.....	12 60.0	+28 01	36.19	51.03	74	1.5	0.55

NOTE.—Units of right ascension are hours and minutes, and units of declination are degrees and arcminutes (J2000).

^a CID = 7: Two adjacent fields; the smaller lies north of the larger and runs nearly along the east edge.

^b CID = 35: Overlap with CID = 36 in southwest corner.

^c CID = 36: Overlap with CID = 35 in northeast corner. The region is 19:02 east-west and 28:53 north-south, centered at (05^h43^m6, −25°45'), and was excluded from this field.

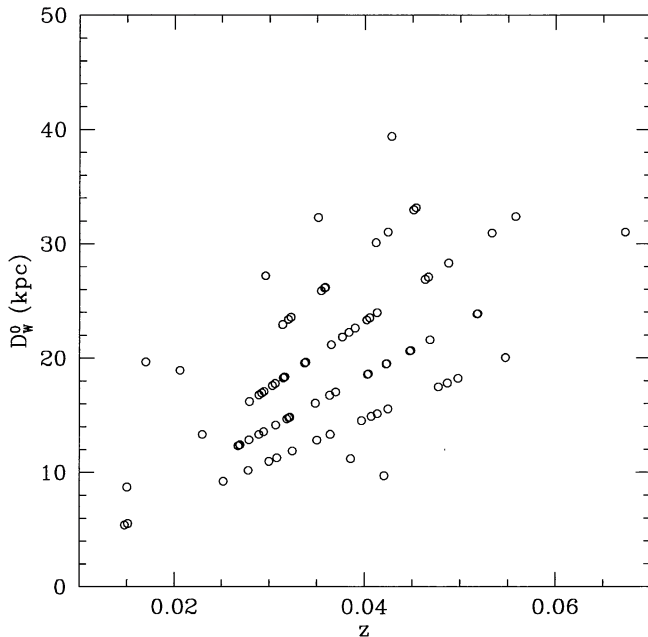


FIG. 9.—Relation between cluster redshift and the cutoff diameter D_W^0 in units of kiloparsecs (for $H_0 = 50 \text{ km s}^{-1} \text{ Mpc}^{-1}$), showing that the selection criterion is effectively a constant cut in angular diameter and thus corresponds to a metric diameter that increases with redshift.

would expect such subsamples to omit more objects with small diameters, leading to larger values of the cutoff diameter. This is borne out by using a preliminary, stringently chosen list of our highest quality distance indicators (Saglia et al. 1996). With this whittled-down subsample, which is 55% of the original list, the mean $\log D_W^0$ increases by only 0.1 while δ_W changes insignificantly, showing the insensitivity of the selection function to large changes in the sample.

A maximum likelihood fitting method is to be used to determine the galaxy distances, and since this technique fits a probability distribution to all observables, this provides additional explicit and implicit selection criteria besides

$S_j(D_W)$. The final values that we use will be given in subsequent papers, but examples of these with preliminary values are as follows: the lower cutoff in the velocity dispersion at $\sigma < 140 \text{ km s}^{-1}$ due to the resolution of the instruments is an explicit limit (Wegner et al. 1996), while the mean surface brightness, $23.39 \text{ mag arcsec}^{-2} \geq \langle SB_e \rangle \geq 16.84 \text{ mag arcsec}^{-2}$, and the smallest effective radius, $R_e \geq 1''.5$, we have observed in our sample are implicit limits (Saglia et al. 1996).

5. CONCLUSIONS

The EFAR project is aimed at measuring the properties and peculiar motions of elliptical galaxies in clusters selected in two regions at distances of 6000–15,000 km s^{-1} . The primary goals of the project are, first, to study the physical properties of a large sample of elliptical galaxies and derive an optimal distance estimator and, second, to determine the bulk motions in the two selected regions in order to establish whether the large-scale coherent motions seen within 6000 km s^{-1} are typical of other regions of the universe, thereby tightening the constraints on cosmological models set by the local velocity field.

There are 84 clusters in our sample, 39 in the region we call Hercules–Corona Borealis (HCB) and 45 on the opposite side of the sky, in the region we call Perseus–Pisces–Cetus (PPC). Most of these clusters lie in the redshift range 6000–15,000 km s^{-1} , with 42 being drawn from the Abell (1958) catalog, 32 from the catalog of Jackson (1982), and a further 10 supplementary clusters found by us on the Sky Survey plates. We have given the redshifts for all of these clusters and shown where they are located with respect to the superclusters identified by Einasto et al. (1994). We find that our sample of Abell (1958) clusters in the range 6000–15,000 km s^{-1} is 92% complete in HCB and 87% complete in PPC.

In these clusters, we have selected 736 candidate elliptical galaxies based on their morphology and apparent size on enlargements of Sky Survey glass copies. Our master list of EFAR galaxies gives the fundamental data, including accurate new positions, for these program galaxies and for 52

calibration galaxies in Coma, Virgo, and the nearby field. In order to quantify our selection criteria, we have measured visual diameters from the Sky Survey enlargements for all the program galaxies (and for the calibration galaxies in Coma) and for a large number of other galaxies in these clusters—a total of 2185 objects. The visual diameters of the program galaxies turn out to correlate with preliminary estimates of the photometric sizes established by subsequent CCD imaging. For each cluster, we are therefore able to characterize the selection criterion for the sample galaxies in terms of these visual diameters. We find that the samples of galaxies in the program clusters are typically 50% complete at 18"–20" and drop from 90% to 10% completeness between 30" and 10".

Subsequent papers in this series will report the spectroscopic and photometric observations, estimate distances and peculiar velocities for the galaxies and clusters, and interpret the implied peculiar velocity field.

G. W. is grateful to SERC and Wadham College for a year's stay in Oxford and to the Alexander von Humboldt–Stiftung for making possible a visit to the Ruhr-Universität in Bochum. M. M. C. acknowledges the support of a Linde-

mann Fellowship, a DIST Collaborative Research Grant, and an Australian Academy of Science/Royal Society Exchange Program Fellowship. R. P. S. acknowledges the support of DFG grants SFB 318 and 375. This work was partially supported by NSF grants AST 90-16930 to D. B., AST 90-17048 and AST 93-47714 to G. W., and AST 90-20864 to R. K. M. and by NASA grant NAG 5-2816 to E. B. The entire collaboration benefited from NATO Collaborative Research Grant 900159 and from the hospitality and monetary support of Dartmouth College, Oxford University, the University of Durham, and Arizona State University. Support was also received from PPARC visitors grants to Oxford and Durham Universities and a PPARC rolling grant: "Extragalactic Astronomy and Cosmology in Durham 1994–1998." The KPNO photographic laboratory produced the extensive set of prints from the Sky Surveys used for measuring galaxy diameters and as finders, which were provided by R. L. D. and D. B.; D. B. measured the positions of all program galaxies using the GASP system, and we extend our great appreciation to the STScI personnel for their help. Josef Wegner compiled the initial sample of candidate galaxies and provided a list of cross-references that proved invaluable.

APPENDIX

CLUSTERS OMITTED FROM THE SURVEY SAMPLE

As of mid-1995, there were 56 Abell clusters with known redshifts and sky positions that would nominally have placed them in the survey sample. The EFAR sample has 34 (61%) of these clusters. The 22 remaining Abell clusters were excluded for the reasons listed below.

Five clusters had redshifts known at the time of the 1986 search but were rejected:

1. *A195*.—Nominal $z = 0.047$. Examination of the POSS print shows that the cluster is much fainter and likely to have $z > 0.05$.
2. *A261*.—Nominal $z = 0.0467$. Examination of POSS prints shows that the quoted redshift is that of a foreground elliptical galaxy. The real Abell cluster is much more distant.
3. *A407*.—Nominal $z = 0.047$; famous "cD in the making," seven galaxies in a common envelope associated with UGC 2489 (see Nilson 1973). We could not obtain good data on each part of this complex system.
4. *A484*.—Nominal $z = 0.0386$. The redshift quoted corresponds to a small radio galaxy near the cluster but not in it. The real Abell cluster is of very faint galaxies in the background.
5. *A539*.—Nominal $z = 0.0267$. This cluster lies at low Galactic latitude, has strong differential reddening, and is in the middle of an emission-line nebula.

Ten clusters did not have redshifts known at the time of the 1986 search and subsequent investigation has indicated that our survey would not have used them:

6. *A256*.—Nominal $cz = 13,379 \text{ km s}^{-1}$. Examination of POSS prints finds a foreground E galaxy superposed on a faint background cluster. Zabludoff et al. (1993) showed this region to have galaxies with cz from 6000 to 30,000 km s^{-1} , but no definite clusters except at the highest cz .
7. *A2995*.—Nominal $cz = 11,332 \text{ km s}^{-1}$. Examination of POSS prints finds three larger galaxies (two spirals, one elliptical) superposed on faint background clusters. Abell (1958) called this cluster distance class 5, making it too far away for our survey. The quoted redshift comes from NED.
8. *A480*.—Nominal $cz = 14,180 \text{ km s}^{-1}$. Struble & Rood (1991) reported this as an incorrect redshift. We confirm this from examination of the POSS print, as we only see a faint cluster, and Abell gave it a distance class of 5.
9. *S0449*.—Nominal $cz = 14,390 \text{ km s}^{-1}$. The redshift is from Dalton et al. (1994) but assigned a probability of 0.05 or less of being correct. Examination of SERC J prints indicates that galaxies in the cluster have $z > 0.1$.
10. *S0471*.—Nominal $cz = 12,891 \text{ km s}^{-1}$. The redshift is from Dalton et al. (1994) but assigned a probability of 0.05 or less of being correct. Examination of SERC J prints indicates that galaxies in the cluster have $z > 0.1$.
11. *A3175*.—Nominal $cz = 11,691 \text{ km s}^{-1}$. The redshift is from Dalton et al. (1994) but assigned a probability of 0.05 or less of being correct. Examination of SERC J prints indicates that galaxies in the cluster have $z > 0.1$.
12. *A2022B*.—Nominal $cz = 9144 \text{ km s}^{-1}$. Examination of POSS prints shows this to be a foreground group to a much fainter Abell cluster. The actual Abell cluster is too distant for our survey.
13. *A2025*.—Nominal $cz = 13,550 \text{ km s}^{-1}$. Examination of POSS prints shows only faint galaxies at the Abell cluster's position. The quoted redshift is probably of a foreground galaxy.

14. *A2506*.—Nominal $cz = 8660 \text{ km s}^{-1}$. The confusing picture given by POSS examination is clarified by Zabludoff et al. (1993), which shows that the galaxies in this region have a large range in redshift. Only the nearest galaxies were used for the quoted redshift. Our survey originally identified a set of galaxies at this redshift as A2506, but these are really a degree away from the Abell cluster's position and are now called the P522-1 group.

15. *A2592*.—Nominal $cz = 13,880 \text{ km s}^{-1}$. Examination of the POSS print finds only faint galaxies. Struble & Rood (1991) stated that this is an incorrect redshift for this cluster.

Two clusters did not have redshifts at the time of our 1986 search and would have been of marginal use for this survey.

16. *A3367*.—Nominal $z = 0.0443$. Examination of POSS prints shows that this cluster is dominated by a cD galaxy, but the other galaxies in the cluster are too faint and too small for our survey. This could be another foreground galaxy-contaminated cluster.

17. *A3374*.—Nominal $z = 0.0471$. Examination of POSS prints shows that this cluster is dominated by a cD galaxy. Only faint galaxies are seen around this cD, too faint for this survey.

Five clusters would have been included in the EFAR survey had we known about their redshifts in 1986:

18. *A154A*.— $cz = 12,837 \text{ km s}^{-1}$.

19. *A295*.— $cz = 12,717 \text{ km s}^{-1}$.

20. *A536*.— $cz = 11,931 \text{ km s}^{-1}$.

21. *A2881*.— $cz = 13,280 \text{ km s}^{-1}$.

22. *A3223*.— $cz = 12,981 \text{ km s}^{-1}$.

REFERENCES

- Aaronson, M., et al. 1989, *ApJ*, 338, 654
 Aaronson, M., Bothun, G., Mould, J., Huchra, J., Schommer, R. A., & Cornell, M. E. 1986, *ApJ*, 302, 536
 Abell, G. O. 1958, *ApJS*, 3, 211
 Abell, G. O., Corwin, H. G., Jr., & Olowin, R. P. 1989, *ApJS*, 70, 1
 Baggle, G., Davies, R. L., Bertschinger, E., Burstein, D., Colless, M. M., McMahan, R. K., Saglia, R. P., & Wegner, G. A. 1993, in *Cosmic Velocity Fields*, ed. F. R. Bouchet & M. Lachièze-Rey (Gif-sur-Yvette: Ed. Frontières), 513
 Bahcall, N. A., & Soneira, R. M. 1984, *ApJ*, 277, 27
 Batuski, D. J., & Burns, J. O. 1985, *ApJ*, 299, 5
 Bender, R., Burstein, D., & Faber, S. M. 1992, *ApJ*, 399, 462
 Bertschinger, E. 1990, in *Particle Astrophysics: The Early Universe and Cosmic Structures*, ed. J. M. Alimi et al. (Gif-sur-Yvette: Ed. Frontières), 411
 Bertschinger, E., Dekel, A., Faber, S. M., Dressler, A., & Burstein, D. 1990, *ApJ*, 364, 370
 Bertschinger, E., & Juskiewicz, R. 1988, *ApJ*, 334, L59
 Burstein, D. 1990, *Rep. Prog. Phys.*, 53, 421
 Burstein, D., Faber, S. M., & Dressler, A. 1990, *ApJ*, 354, 18
 Burstein, D., & Heiles, C. 1982, *AJ*, 87, 1165
 ———, 1984, *ApJS*, 54, 33
 Colless, M. M. 1995, *AJ*, 109, 1937
 Colless, M. M., Burstein, D., Wegner, G., Saglia, R. P., McMahan, R., Davies, R. L., Bertschinger, E., & Baggle, G. 1993, *MNRAS*, 262, 475
 Colless, M. M., & Dunn, A. M. 1996, *ApJ*, 458, 435
 Courteau, S., Faber, S. M., Dressler, A., & Willick, J. A. 1993, *ApJ*, 412, L51
 Dalton, G. B., Efstathiou, G., Maddox, S. J., & Sutherland, W. J. 1994, *MNRAS*, 269, 151
 Davies, R. L., Baggle, G., Bertschinger, E., Burstein, D., Colless, M. M., McMahan, R., Saglia, R., & Wegner, G. A. 1993, in *Structure, Dynamics and Chemical Evolution of Elliptical Galaxies*, ed. I. J. Danziger, W. W. Zeilinger, & K. Kjar (Garching: ESO), 159
 de Carvalho, R. R., & Djorgovski, S. 1992, *ApJ*, 389, L49
 Dekel, A. 1994, *ARA&A*, 32, 371
 Dekel, A., et al. 1996, in preparation
 Djorgovski, S., & Davis, M. 1987, *ApJ*, 313, 59
 Dressler, A. 1984, *ApJ*, 281, 512
 Dressler, A., Faber, S. M., Burstein, D., Davies, R. L., Lynden-Bell, D., Terlevich, R. J., & Wegner, G. 1987a, *ApJ*, 313, L37
 Dressler, A., Lynden-Bell, D., Burstein, D., Davies, R. L., Faber, S. M., Terlevich, R. J., & Wegner, G. 1987b, *ApJ*, 313, 42
 Einasto, M., Einasto, J., Tago, E., Dalton, G. B., & Andernach, H. 1994, *MNRAS*, 269, 301
 Faber, S. M., & Burstein, D. 1988, in *Large-Scale Motions in the Universe*, ed. V. C. Rubin & G. C. Coyne (Princeton: Princeton Univ. Press), 115
 Faber, S. M., Wegner, G., Burstein, D., Davies, R. L., Dressler, A., Lynden-Bell, D., & Terlevich, R. J. 1989, *ApJS*, 69, 763
 Feldman, H. A., & Watkins, R. 1994, *ApJ*, 430, L17
 Fetisova, T. S. 1982, *Soviet Astron.—AJ*, 25, 647
 Freudling, W., da Costa, L. N., Wegner, G., Giovanelli, R., Haynes, M. P., & Salzer, J. J. 1995, *AJ*, 110, 920
 Gregg, M. D. 1992, *ApJ*, 384, 43
 ———, 1995, *ApJ*, 443, 527
 Guzman, R., & Lucey, J. R. 1993, *MNRAS*, 263, L47
 Han, M., & Mould, J. R. 1990, *ApJ*, 360, 448
 Jackson, R. 1982, Ph.D. thesis, Univ. California, Santa Cruz
 Jacoby, G. H., et al. 1992, *PASP*, 104, 599
 Jørgensen, I., Franx, M., & Kjærgaard, P. 1993, *ApJ*, 411, 34
 Kaiser, N. 1988, *MNRAS*, 231, 149
 ———, 1991, *ApJ*, 366, 388
 Lauer, T. R., & Postman, M. 1994, *ApJ*, 425, 418
 Lucey, J. R., Guzman, R., Carter, D., & Terlevich, R. J. 1991, *MNRAS*, 253, 584
 Lynden-Bell, D., Faber, S. M., Burstein, D., Davies, R. L., Dressler, A., Terlevich, R. J., & Wegner, G. 1988, *ApJ*, 326, 19
 Malmquist, K. G. 1920, *Medd. Lunds Astron. Obs.* II, No. 22
 Mathewson, D. S., & Ford, V. L. 1994, *ApJ*, 434, L39
 Mathewson, D. S., Ford, V. L., & Buchhorn, M. 1992, *ApJ*, 389, L5
 Mould, J. R., Akeson, R. L., Bothun, G. D., Han, M., Huchra, J. P., Roth, J., & Schommer, R. A. 1993, *ApJ*, 409, 14
 Neyman, J., & Scott, E. L. 1959, in *Handbuch der Physik*, 53, ed. S. Flügge (Berlin: Springer), 416
 Nilson, P. 1973, *Uppsala General Catalogue of Galaxies*, Uppsala Astron. Obs. Ann., 6, 72
 Pahre, M. A., Djorgovski, S. G., & de Carvalho, R. R. 1995, *ApJ*, 453, L17
 Postman, M., & Lauer, T. R. 1995, *ApJ*, 440, 28
 Primack, J. R., Olivier, S., Blumenthal, G. R., & Dekel, A. 1991, in *ASP Conf. Proc. 15, Large-Scale Structures and Peculiar Motions in the Universe*, ed. D. W. Latham & L. A. N. da Costa (San Francisco: ASP), 251
 Riess, A. G., Press, W. H., & Kirshner, R. P. 1995, *ApJ*, 445, L91
 Saglia, R. P., Baggle, G., Bertschinger, E., Burstein, D., Colless, M. M., Davies, R. L., McMahan, R. K., & Wegner, G. 1996, in preparation (Paper III)
 Saglia, R. P., Bender, R., & Dressler, A. 1993a, *A&A*, 279, 75
 Saglia, R. P., Bertschinger, E., Baggle, G., Burstein, D., Colless, M. M., Davies, R. L., McMahan, R. K., & Wegner, G. 1993b, *MNRAS*, 264, 961
 Seljak, U., & Bertschinger, E. 1994, *ApJ*, 427, 523
 Silk, J. 1989, *ApJ*, 342, L5
 Smoot, G. F., et al. 1992, *ApJ*, 396, L1
 Strauss, M. A., & Willick, J. A. 1995, *Phys. Rep.*, 261, 271
 Struble, M. F., & Rood, H. J. 1987, *ApJS*, 63, 543
 ———, 1991, *ApJS*, 77, 363
 Tully, R. B., & Fisher, J. R. 1987, *Nearby Galaxies Atlas* (Cambridge: Cambridge Univ. Press)
 Tully, R. B., Scaramella, R., Vettolani, G., & Zamorani, G. 1992, *ApJ*, 388, 9
 Vittorio, N., Juskiewicz, R., & Davis, M. 1986, *Nature*, 323, 132
 Watkins, R., & Feldman, H. A. 1995, *ApJ*, 453, L73
 Wegner, G., Davies, R. L., Baggle, G., Saglia, R. P., McMahan, R. K., Colless, M. M., Burstein, D., & Bertschinger, E. 1996, in preparation (Paper II)
 Wegner, G., Davies, R. L., Colless, M. M., Burstein, D., Bertschinger, E., & McMahan, R. K. 1991, in *ASP Conf. Proc. 15, Large-Scale Structures and Peculiar Motions in the Universe*, ed. D. W. Latham & L. A. N. da Costa (San Francisco: ASP), 129
 Willick, J. A. 1990, *ApJ*, 351, L5
 ———, 1991, Ph.D. thesis, Univ. California, Berkeley
 ———, 1994, *ApJS*, 92, 1
 Zabludoff, A. I., Geller, M. J., Huchra, J. P., & Vogeley, M. S. 1993, *AJ*, 106, 1273
 Zucca, E., Zamorani, G., Scaramella, R., & Vettolani, G. 1993, *ApJ*, 407, 470